



Slovenska Fuzijska Asociacija  
Slovenian Fusion Association

Association EURATOM - MHEST  
**ANNUAL REPORT 2005**

Ljubljana, December 2006





Slovenska Fuzijska Asociacija  
Slovenian Fusion Association

# Association EURATOM - MHEST ANNUAL REPORT 2005

The Annual Report 2005 of the Association EURATOM-MHEST  
covers the period 1 January to 31 December 2005

Compiled by Milan Čerček and Bojan Žefran  
This work, supported by the European Communities under the  
contract of Association between EURATOM and MHEST, was  
carried out within the framework of the European Fusion  
Development Agreement (EFDA). The views and opinions  
expressed herein do not necessarily reflect those  
of the European Commission.

Association EURATOM-MHEST

Institute Jožef Stefan  
Jamova 39  
SI-1000 Ljubljana  
Tel. +386 1 5885 450  
<http://www.sfa-fuzija.si>



## CONTENTS

<b>1. Introduction</b>	1
1.1. General Information	2
1.2. Financial Information	3
1.3. Statistics	4
<b>2. Fusion Physics Programme</b>	
2.1. Interaction of vibrationally excited Hydrogen with Fusion Relevant Materials	5
2.2. Heterogeneous Surface Recombination of Neutral Hydrogen Atoms on Fusion Relevant Materials	13
2.3. Analysis of Narrow Support Element of the W7-X Magnet System under Design Loads	21
2.4. Application of Ion Beam Analytical Methods to the Studies of Plasma Wall Interaction in Tokamaks	29
2.5. Collaboration in DEMO Working Group	35
<b>3. Underlying Technology Programme</b>	
3.1. Gas Impermeable Coating for SiC <sub>f</sub> /SiC	41
3.2. Novel Processing of SiC/SiC by Slip-infiltration of SiC Fibre Pre-forms with SiC under Vacuum	47
<b>4. Fusion Technology Programme</b>	
4.1. 2D and 3D Deterministic Transport, Sensitivity and Uncertainty Analysis of HCPB Tritium Breeder Module Mock-up Benchmark	53
4.2. Analysis, Design and Manufacture of Local Machining Tool for Blanket Module Flexible Support Housing	59
<b>5. Public Information</b>	61
<b>6. Publications</b>	63



## 1. Introduction

The Slovenian Fusion Association was founded on 1 January 2005 with the signing the Contract of Association between European Commission, representing EURATOM, and Ministry of Higher Education, Science and Technology of the Republic of Slovenia. From the very beginning the efforts of the institutions willing to join the European fusion programme were also supported by the Slovenian Research Agency, which included the fusion research among priority themes of the Slovenian research programme.

The contributions of the institutions in the Association to the several areas of the fusion programme are based on R&D experiences of the researchers in the fields of nuclear, atomic and plasma physics, ceramic materials development, mechanical engineering and computer aided design. The major equipment available in the institutions includes the following: an ion beam accelerator with materials diagnostic installations, a TRIGA reactor, an advanced dedicated fully-integrated high resolution microscope facility for nanostructural materials, computer systems for simulations, structural mechanical analyses and CAD, etc.

These areas in the programme are:

- Plasma-surface interaction in ITER-relevant conditions. The tasks, dealing with interaction of molecular and atomic hydrogen/deuterium with fusion-relevant materials fit very well into the programme of PWI TF.
- The development of new ceramic materials for fusion reactors. The research in the Association is performed within EFDA Underlying Technology Programme.
- Analyses of TBM neutronics experiments and validation of EFF nuclear cross section data. The collaboration in this area of EFDA Technology programme started as cost sharing actions already in 2001.
- The development and manufacture of a special tool for the construction and production of ITER parts.
- Carrying out structural mechanical analyses and evaluations to support Wendelstein 7X project.

The Association also collaborates in the DEMO Working Group, contributing in the topics related to the conventional NPP technology, in particular in the topics related to nuclear safety and nuclear waste treatment. There is a substantial expertise available, derived from the long-standing fission programme in the country.

Great care is given in the Association to improving the public awareness for fusion energy research. The central event in 2005, organized by the Association in collaboration with EFDA and the European Commission, was the exhibition called “FUSION EXPO - Fusion, energy for the future”, which took place in Ljubljana from 21 March to 1 April.

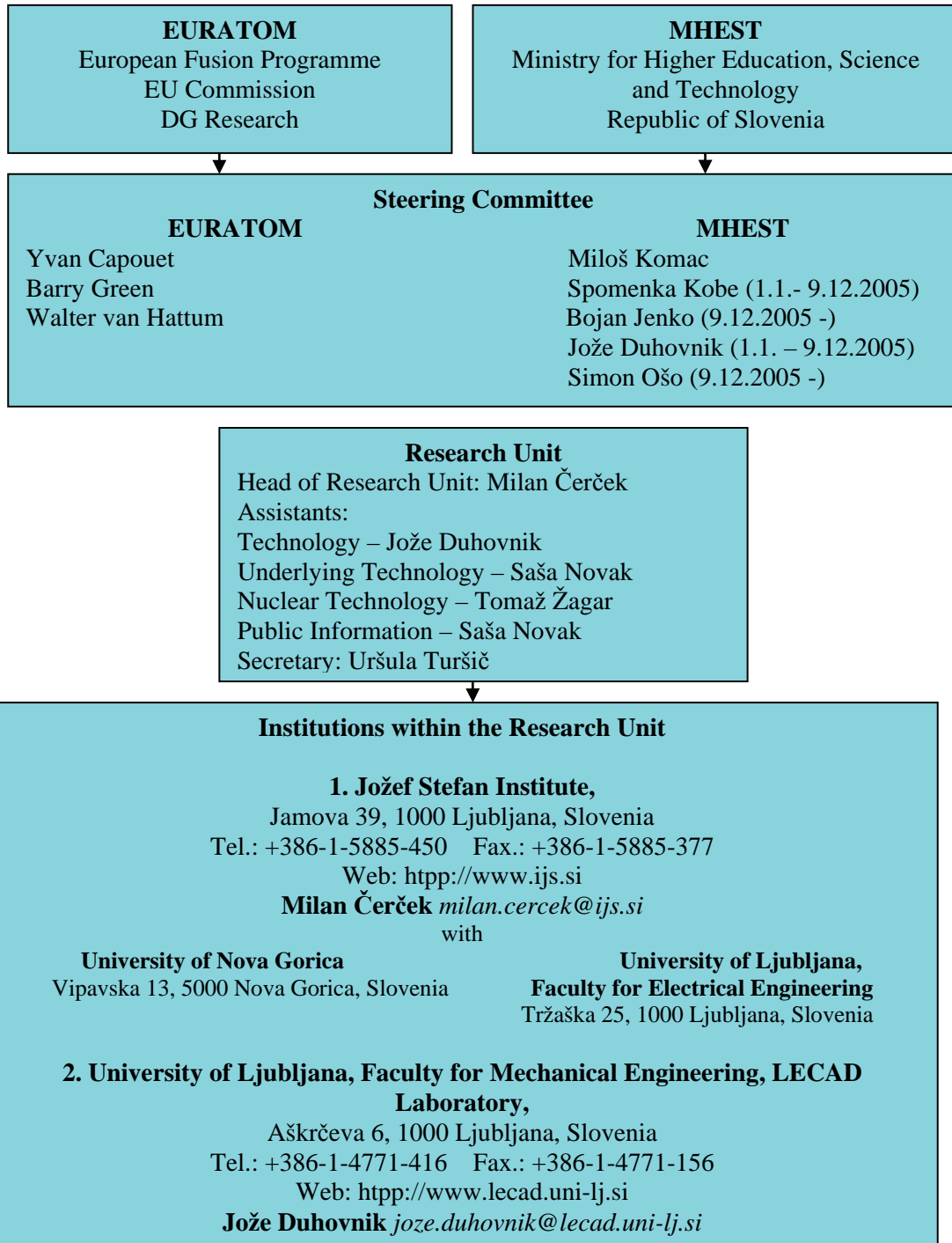
After the first year of work in the frame of the Slovenian Fusion Association, the researchers are committed to intensify their collaboration in the European fusion programme, which will be possible only by a continuing cooperation of individuals and institutions, who have so kindly given the support from the very beginning.



Milan Čerček  
Head of Research Unit

## 1.1. General Information

### Association EURATOM-MHEST Management structure



## Slovenian representatives in the European committees relevant to fusion research and development

### Consultative Committee for the EURATOM Specific Programme on Nuclear Energy Research – Fusion (CCE-FU)

Miloš Komac      Ministry for Higher Education, Science and Technology of Republic of Slovenia

Milan Čerček      Head of Research Unit, Jožef Stefan Institute, Ljubljana

### EFDA Steering Committee

Jože Duhovnik      University of Ljubljana

### EFDA Scientific and Technical Advisory Committee (STAC)

Milan Čerček      Head of Research Unit, Jožef Stefan Institute, Ljubljana

### EFDA Administrative and Financial Advisory Committee (AFAC)

Darko Korbar      Jožef Stefan Institute, Ljubljana

### Public Information Group

Saša Novak      Jožef Stefan Institute, Ljubljana

## 1.2. Financial Information

Table 1.1 Expenditure for 2005

	Expenditure (Euro)
<b>General Support</b> (20% EU contribution)	<b>970,514</b>
Physics	665,419
Underlying Technology	305,095
<b>EFDA</b> (20% EU contribution)	<b>48,216</b>
Technology	48,216
<b>Mobility</b> (100% EU contribution)	<b>6,979</b>
<b>TOTAL</b>	<b>1,025,709</b>

### 1.3. Statistics

Table 1.2 R&D projects in the Association EURATOM-MHEST for 2005

	JSI	ULJ	
<b>Physics</b>	4	1	<b>5</b>
<b>Underlying Technology</b>	2	-	<b>2</b>
<b>Technology</b>	1	1	<b>2</b>
<b>TOTAL</b>	7	2	<b>9</b>

Table 1.3 Manpower for 2005

	Professional	Non professional	TOTAL
JSI	27	9	36
ULJ	4	0	4
	<b>31</b>	<b>9</b>	<b>40</b>

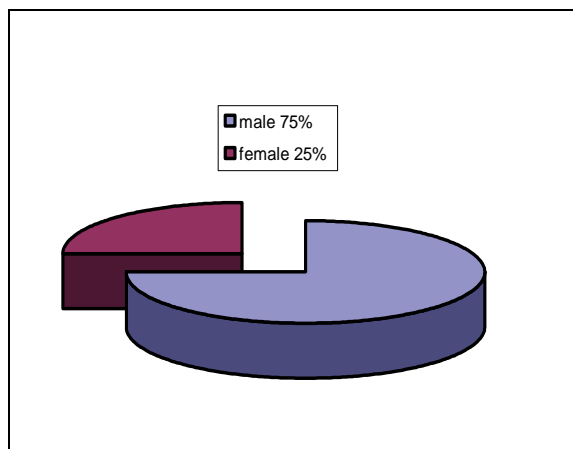


Figure 1. Association EURATOM-MHEST staff in 2005 by gender

## Interaction of vibrationally excited hydrogen with fusion relevant materials

**Iztok Čadež, Milan Čerček, Zvone Grabnar, Sabina Markelj, Primož Pelicon, Dušan Rudman, Zdravko Rupnik**

“Jožef Stefan” Institute, Ljubljana  
 iztok.cadez@ijs.si,

**Tomaž Gyergyek**  
 Faculty for Electrical Engineering, University of Ljubljana

**Vida Žigman**  
 University of Nova Gorica

### 1 INTRODUCTION

The main goal of this project is to provide quantitative data on processes with vibrationally excited hydrogen molecules that are needed for modelling fusion edge plasma and plasma-wall interaction. We also search for specific phenomena with such molecules that might have high cross sections. The isotope effect in these processes is studied as heavy hydrogen isotopes are important for fusion application and also as such studies lead to deeper insight into the reaction dynamics itself. In the following we will use abbreviation H2V for any isotopomer of vibrationally excited hydrogen molecule, e.g. H<sub>2</sub>, HD, D<sub>2</sub>.

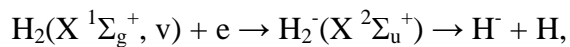
In particular we are interested in the following processes at the surface of fusion relevant materials:

- Vibrational distribution of molecules released from surfaces due to thermal desorption and recombinative desorption for different surface temperatures and composition.
- Ratio of atomic to molecular species released from a surface and its variation with surface parameters.
- Interaction of vibrationally excited molecules with plasma-facing materials:
  - Change of vibrational distribution caused by interaction with the surfaces.
  - Transfer of vibrational energy to the wall and its effects on erosion yields.
  - Wall sticking probability for the excited molecules.

Due to the importance of the volume reactions in divertor plasma we are also interested in:

- Binary collisions of vibrationally excited hydrogen molecules with other atomic particles.

We are using unique method for vibrational spectroscopy of hydrogen molecules that allows us new and original experiments. This diagnostic technique is based on the properties of the dissociative electron attachment (DEA) in H<sub>2</sub>:



and similar in other isotopomers. This, lowest energy DEA in hydrogen occurs at electron energy around 4 eV for molecules in the ground vibrational state. Its main characteristics are:

- Very strong rise of the cross section with vibrational and rotational excitation of the target molecule (reaching 10<sup>-15</sup> cm<sup>2</sup> range for high v!).

- Vertical H<sup>-</sup> (D<sup>-</sup>) onset at the DEA threshold and production of low-energy ions,
- DEA threshold for excited molecule is displaced by internal excitation energy towards lower energy,
- Pronounced isotope effect for low v.

The method for hydrogen vibrational spectroscopy based on the DEA was originally developed at Université Pierre et Marie Curie, Paris in the late 80ties.

The present project “Interaction of Vibrationally Excited Hydrogen with Fusion Relevant Materials” (P2) is a continuation of the previous Cost Shearing Project (CSP) which was terminated in June 2005 [2].



Figure 1: The vibrational spectrometer is housed in the vacuum chamber between Helmholtz coils that generate the homogeneous magnetic field needed for e-beam collimation and ion extraction.

Within this project we have developed a new experimental set-up (DTVE-B) for the vibrational spectroscopy of hydrogen molecules that is shown in figures 1 and 2. It employs an original extraction system [4] for light negative ions (H<sup>-</sup> and D<sup>-</sup>) using an electrostatic field penetration technique in the presence of homogenous magnetic field. Some new data on DEA in H<sub>2</sub> and D<sub>2</sub> were acquired [5].

During CSP we also developed and tested procedures for quantitative depth profiling of H and D in materials [1], [6]. For this we use an analysis of the energy spectra of ejected H and D after the studied sample is irradiated by a high energy <sup>7</sup>Li<sup>2+</sup> ion beam. This Ion Beam Analytical (IBA) method called ERDA (Elastic Recoil Detection Analysis) is set at 2MV tandem accelerator in our laboratory. By using ERDA we have performed initial in situ and in real time studies of the interaction of neutral hydrogen atoms and molecules (H, D, H<sub>2</sub> and D<sub>2</sub>) with W and Ti [13]. For these studies we employed a specially designed hydrogen exposure cell (HEC).

Also, during the CSP we continued modelling studies of plasma that is relevant to edge conditions in tokamaks and to the negative ion sources [7], [8], [9].

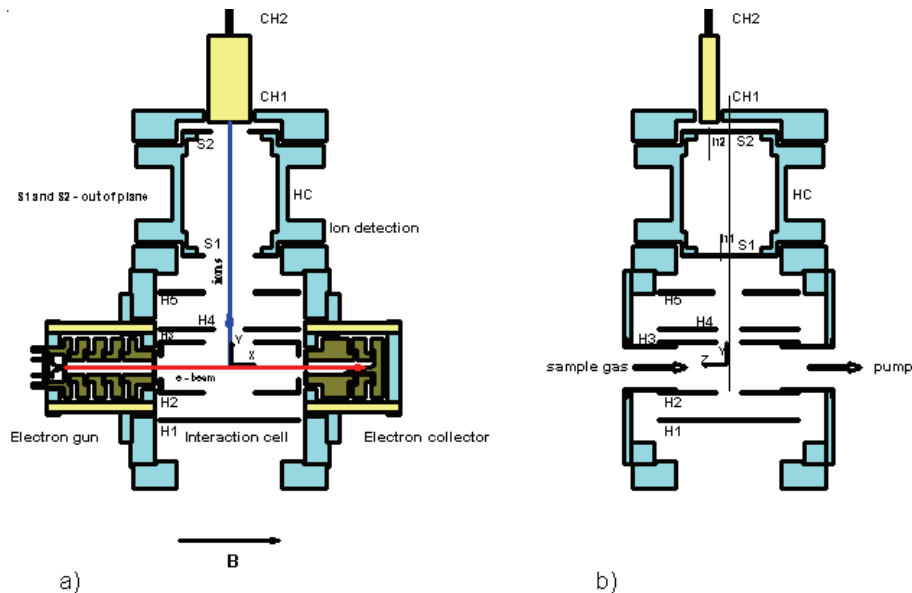


Figure 2: Electrode system of the hydrogen vibrational spectrometer (DTVE-B): a) horizontal and b) vertical cut.

## 2 WORK PERFORMED IN THE SECOND HALF OF 2005

Work on the project P2 is a continuation of the mentioned CSP and follows the same objectives. Activities during the second half of 2005 followed four main subtasks.

### 2.1 Vibrational diagnostics

The vibrational spectroscopy method was further developed in order to improve the energy resolution. Low resolution electron gun (shown in figure 2a) was replaced by a trochoidal electron monochromator and measurements were performed at lower extraction voltages than before. In this way a notable increase in resolution was achieved [10].

In order to study the vibrational states of molecules created by recombination we have constructed two permeation sources to be inserted close to the interaction region of DTVE-B. One permeation source comprises 0.1 mm thick Pd membrane and another one 0.25 mm Ta membrane. Thermocoax heater is coiled around 10mm diameter membrane holder. The source temperature was varied from room temperature up to 320 °C. An initial study of permeation through Pd membrane showed that only molecules in the ground vibrational state are produced when 1 bar pressure of hydrogen is applied to the membrane. The studies with Ta were not yet finished due the Ta membrane contamination during assembly soldering.

### 2.2 Test atmospheres with H<sub>2</sub>V

A test source (TS) for production of H<sub>2</sub>Vs was assembled. A drawing of the TS is shown in figure 3 as it is mounted on the top of detection block of DTVE-B. It is made of copper and has cylindrical shape. Air, water or LN<sub>2</sub> flow can cool the top part of the TS.

Hydrogen is caused to flow through the TS and it is partially dissociated by the hot tungsten filament that is mounted inside the TS. A tantalum disk was mounted on the cold finger that is facing the exit orifice directed towards the interaction region of DTVE-B. Molecules formed by the atom recombination on the Ta disc are vibrationally excited and together with unperturbed gas flow to the interaction region where they are intersected by the probing e-beam.

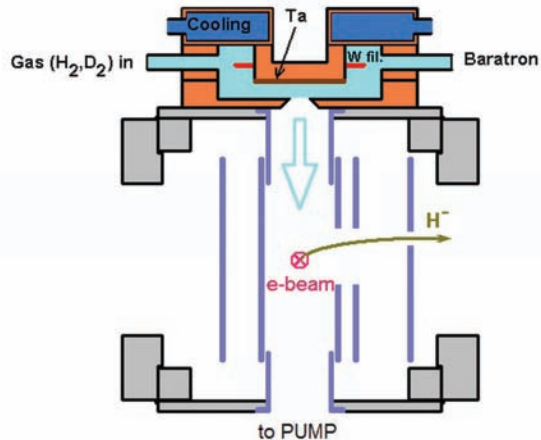


Figure 3: Test source of H<sub>2</sub>Vs as mounted in DTVE-B.

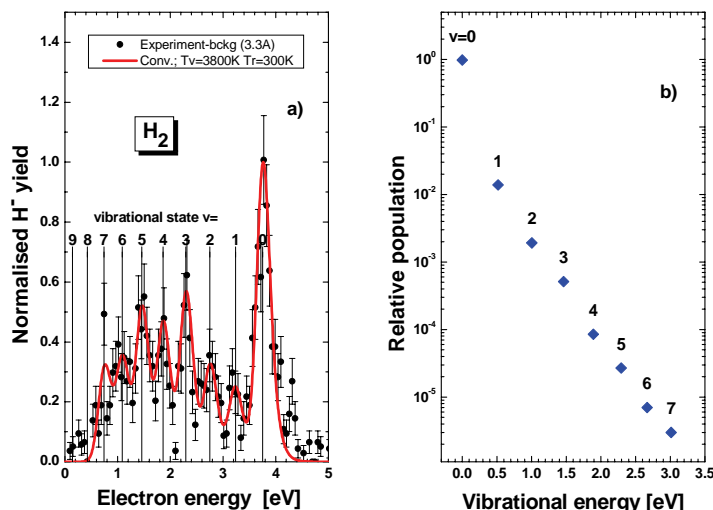


Figure 4: Experimental and fitted spectrum of H<sub>2</sub>V created by recombination on Ta (a) and deduced relative populations of different vibrational states (b).

An example of vibrational spectrum is shown in figure 4a. Experimental spectrum of H<sup>+</sup> yield vs. electron energy is fitted by an appropriate deconvolution procedure that enables determination of vibrational state populations as shown in figure 4b. High vibrational (3800K) and relatively low rotational (300 K) temperatures were obtained, which is in agreement with previous similar measurements with Ta.

A low relative population of vibrationally excited fraction in the gas flow is mostly due to the low dissociation rate of the hydrogen atmosphere in the cell. This can be significantly

increased by larger hot-W area or by discharge technique leading to a higher flux of excited molecules.

The physical basis for modelling vibrational kinetics in hydrogen as applied to the specific conditions in the hydrogen cell with hot tungsten filament was analysed and established. The hydrodynamic approach has been foreseen as more suitable than the kinetic. An alternative approach by Monte Carlo simulation was also considered.

### 2.3 Hydrogen plasma

Further reconstruction of the existing magnetised plasma machine was performed in order to facilitate the production of hydrogen negative ions. The vacuum chamber has been divided into three compartments with differential pumping. In this way lower pressures were obtained in the source region, and plasma with a substantial part of high energy electrons is produced. They are needed for excitation of hydrogen molecules into vibrational and other highly excited states. In the experimental region higher pressures were obtained, appropriate for production of negative ions. A Langmuir probe diagnostic system was improved for measurements in negative ion plasma. An additional diagnostic system for negative ions was developed based on an electron photodetachment method. A Nd-Yag laser with the wavelength 1064 nm, which produces 5 ns long pulses with 28 mJ of energy, is used together with a Langmuir probe. The repetition rate of the pulses can be adjusted to maximum 15 Hz. During the preliminary measurements we detected a photoablation signal from the probe. The phenomenon is similar to that obtained very recently in the experiments in divertor simulators [Kajita S. et al., CONTRIB PLASM PHYS 44 (7-8): 607 2004 ]. Further study of it is necessary. A substantial part of the work was performed within the frame of a graduation thesis [16].

We have continued the computer simulation of a bounded hydrogen plasma system with positive and negative ions and energetic electrons. It was found that in such plasma with 3 groups of negative particles (cool electrons, hot electrons and negative ions) spontaneous formation of potential barriers is possible. Such localised potential drops (double layers) prevent less energetic negative particles from entering into the region with more negative potential and, on the other hand, accelerate positive ions to higher velocities with which they hit into the electrodes.

We have continued also with theoretical modelling of sheath formation in front of a negative electron emitting electrode in the presence of energetic electrons in the hydrogen plasma [11], [2], [3]. We have developed a fluid and a kinetic model of this problem. Both models predict two possible plasma potentials in front of the electrode, which again means that double layer structures are formed in the plasma. Our fluid model predicts also that when electron emission from the electrode is critical, the current voltage characteristics of such an electrode can have up to three zeros. This means that the current collected by the electrode can have zero values at three different biases of the electrode or, that very high values of the electrode floating potential are possible.

### 2.4 Hydrogen depth profiling

Data from the first measurements with HEC (Lunca) [13] were analysed with special emphasise on surface-to-bulk and bulk diffusion and error estimation. The problems that we previously had with vacuum tightness in the cooling line were corrected by constructing the new envelope of the cell.

### 3 INTERNATIONAL COLLABORATION

In order to enhance integration of our activities into the current research in the field of edge plasma and plasma-surface interaction of European fusion community we started close mutual exchange of information especially with FZ Jülich. Common meeting “*1<sup>st</sup> bilateral meeting on plasma edge physics and plasma-wall interaction Forschungszentrum Jülich - Jožef Stefan Institute*, Jülich, 28-29 September 2005, was organized and activities of Slovenian Fusion Association, including project P2 [13],[14], were discussed.

We are also participating in the EFDA Task Force for Plasma Wall Interaction ([www.efda-taskforce-pwi.org](http://www.efda-taskforce-pwi.org)) and presented the current status of all (including P2) PWI activities within SFA at the 4<sup>th</sup> annual meeting in Cadarache, 17-19 October 2005 [15].

## PUBLICATIONS

### Original articles

- [1] Pelicon P., Razpet A., Markelj S., Čadež I., Budnar M., *Elastic recoil detection analysis of hydrogen with  $^7\text{Li}$  ions using a polyimide foil as a thick hydrogen reference*. Nucl. instrum. methods phys. res., B Beam interact. mater. atoms. **227** (2005) pp 591-596.
- [2] Gyergyek T. and Čerček M., *Fluid model of a sheath formed in front of an electron emitting electrode immersed in a plasma with two electron temperatures*. Contrib. Plasma Phys., **45** (2005) pp 89-110.
- [3] Gyergyek T., Čerček M.; *Sheath in front of a negatively biased collector that emits electrons and is immersed in a two electron temperature plasma*, Contrib. Plasma Phys., **45** (2005), 568-581.

### Conference papers

- [4] Markelj S., Rupnik Z., I. Čadež I., *Vibrational spectroscopy of hydrogen molecules: Extraction of hydrogen ions by field penetration technique in the presence of perpendicular magnetic field*, XXVIIth ICPIG, Eindhoven, the Netherlands, 18-22 July, 2005, Proceedings 08-237.
- [5] Čadež I., Rupnik Z. and Markelj S., *Cross section for dissociative electron attachment to  $\text{H}_2$  and  $\text{D}_2$* , ibid., Proceedings 02-236.
- [6] Čadež I., Razpet A., Pelicon P., Markelj S., and Brezinsek S., *ERDA analysis of hydrogen and deuterium in the plasma-exposed graphite surfaces from the tokamak TEXTOR*, 17<sup>th</sup> International Conference on Ion Beam Analysis, June 26- July 1, 2005, Sevilla, Spain.
- [7] Čerček M., Gyergyek T., *Double layer formation in a negative ion plasma with a bi-Maxwellian electron distribution*, 32nd EPS Conference on Plasma Physics (EPS 2005), 27 June - 1 July, 2005, Tarragona, Spain.
- [8] Gyergyek T., Čerček M.; *Sheath formation in a two-electron temperature plasma*, 32nd EPS Conference on Plasma Physics (EPS 2005), 27 June - 1 July, 2005, Tarragona, Spain.
- [9] Gyergyek T., Čerček M.; *Sheath formation in front of a negatively biased electrode immersed in a two electron temperature plasma*, XXVIIth ICPIG, Eindhoven, the Netherlands, 18-22 July, 2005.

- [10] Markelj S., Rupnik Z. and Čadež I., *Detection system for vibrational spectroscopy of hydrogen molecules for studies of collision processes in fusion edge plasma*, International Conference Nuclear Energy for New Europe 2005, Bled, Slovenia, 5 - 8 September 2005.
- [11] Gyergyek T., Čerček M.; *Multiple solutions for the sheath potential drop in front of a floating electron emitting collector immersed in a two electron temperature plasma*, International Conference Nuclear Energy for New Europe 2005, Bled, Slovenia, 5 - 8 September 2005.

## Reports

- [12] Čadež I., Čerček M., Grabnar Z., Gyergyek T., Markelj S., Mihelič M., Pelicon P., Razpet A., Rupnik Z., *Interaction of vibrationally excited hydrogen with fusion relevant materials: final report*, (EURATOM, FU06-CT-2003-00010), 2005 pp 1-23.
- [13] Markelj S., Čadež I., Pelicon P., Rupnik Z., *In situ studies of interaction of thermal hydrogen molecules and atoms with W, graphite and some other materials*: presented at 1st Bilateral Meeting on Plasma Edge Physics and Plasma-Wall Interaction, 28-30 September, 2005, Forschungszentrum Jülich.
- [14] Čadež I., Markelj S., Rupnik Z., Čerček M., Gyergyek T., Žigman V., *Experiments with vibrationally excited hydrogen molecules ( $H_2, D_2$ ) of relevance for edge plasmas and plasma wall interaction*: presented at 1st Bilateral Meeting on Plasma Edge Physics and Plasma-Wall Interaction, 28-30 September, 2005, Forschungszentrum Jülich.
- [15] Čadež Iztok et al., *Activities relevant to PWI in fusion devices of Slovenian Fusion Association (SFA) (Association EURATOM - MHST)*: presented at 4th Meeting of EFDA Task Force for Plasma Wall Interaction, 17-19 October, 2005, Cadarache, France. 2005, ([http://130.183.3.16/efda/\\_\\_files/File/ppt/cadezi\\_4thm\\_tfpwi.ppt](http://130.183.3.16/efda/__files/File/ppt/cadezi_4thm_tfpwi.ppt)).

## Theses

- [16] Maglica J., *Production and characterization of hydrogen plasma*, grad. thesis, University of Ljubljana 2005, (in slovenian).



## Heterogeneous Surface Recombination of Neutral Hydrogen Atoms on Fusion Relevant Materials

**Miran Mozetič, Aleksander Drenik, Tatjana Filipič, Janez Kovač,  
Janez Trtnik, Alenka Vesel**

“Jožef Stefan” Institute  
Department Surface Engineering and Optoelectronics  
Plasma Laboratory  
[miran.mozetic@ijs.si](mailto:miran.mozetic@ijs.si)

### 1 INTRODUCTION

Neutral hydrogen, deuterium and tritium atoms (hereafter: H atoms) are present in the cold edge and divertor plasmas in tokamaks as well as in vacuum components between the divertor and the pumps. The atoms in the plasma edge and divertor regions take part in a variety of collision processes. Hydrogen atoms form molecules with elements of plasma - facing components, presently predominating hydrocarbons arising from carbon surfaces, as well as with impurities on other surfaces. Unlike molecules that would not react with carbon even at elevated temperature, hydrogen atoms are reactive already at room temperature. It applies not only for hot protons coming from plasma but also for cold atoms that are found in the plasma edge layer. Slow atoms were detected in the plasma edge layer of a tokamak with several different diagnostic methods. Measurements in TEXTOR-94 showed that the atomic hydrogen flux from the carbon, deduced from Balmer line  $H_\alpha$  measurements, is comparable to molecular flux at low carbon temperature. By heating of the test limiter surface the molecular intensity dropped and the intensity of atomic species increased. At high temperatures (above carbon temperature of 1500K) the atomic release dominates and molecules are practically negligible. Such behaviour was also found in ion beam experiments.

In order to estimate the H-atom density in different parts of fusion reactor, it is necessary to have a database on recombination coefficients. There is a lack of reliable data on surface recombination of hydrogen atoms on materials. The recombination coefficients depend on particular experimental conditions like surface morphology (roughness), surface temperature... There seems to be no general rule, but the recombination coefficients tend to increase with increasing temperature and this effect should be taken into account as the materials facing plasma in fusion devices are always heated to high temperature. The goal of the project was to create a database on recombination coefficients including a state of the art and to include our own results. Recombination coefficients were measured for several fusion relevant materials.

### 2 WORK PERFORMED IN 2005

An experimental plasma reactor has been constructed and tested. The reactor has two discharge chambers, one with the volume of 30l and the other with the volume of 3l. A photo of the 30l reactor is shown in Figure 1, while the discharge chamber of the 3l reactor is shown in Figure 2. The reactor is pumped with a two-stage rotary pump with the pumping speed of 63 m<sup>3</sup>/h and the base pressure below 0.1 Pa. Pressure is measured with a precise absolute

gauge and a Pirani gauge. Between the gauges and the discharge chamber there are specially designed recombinators to protect the gauges degradation that might be caused by interaction of plasma radicals with the gauge head. Another, larger recombillator is placed between the discharge chamber and the vacuum pump to prevent degradation of oil during pumping of plasma radicals. The transmission of the recombinators for plasma radicals was measured with thermocouple catalytic probes. Since the flux of radicals through the recombinators was below the detection limit of the probe it was concluded that the recombinators performed well. Plasma is created in the both discharge vessels by inductively coupled RF generator with the frequency of 27.12 MHz and with the power adjustable up to 5kW).

Several probes have been constructed for measuring H density in the plasma reactor. The density was measured in a side vessel of the reactors in order to prevent the probe tips from overheating. The density depended on pressure and discharge power and was of the order of  $10^{21} \text{ m}^{-3}$ . The density was measured also in the remote parts of the experimental system. The density was decreasing with increasing distance from the source, i.e. the discharge vessel. The decrease was higher at higher pressure, while at a pressure below few 10Pa the H density was substantial even close to the pump. In order to recombine the atoms prior to entering the pump itself, we constructed the recombillator as mentioned above.

We also constructed an experimental plasma reactor with DC discharge with the power adjustable up to 21kW. The reactor is under test and will be available for routine work in 2006.

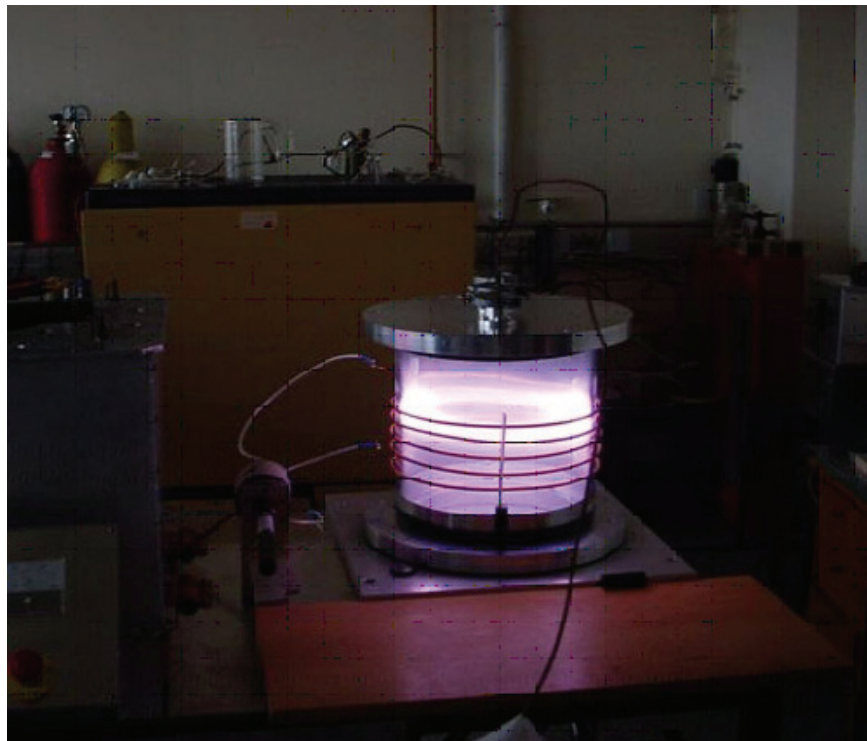


Figure 1: The 30l hydrogen plasma reactor



Figure 2: The discharge chamber of the 3l hydrogen plasma reactor

The main work was done on preparing a database on recombination coefficients. All available data from recent as well as old literature were collected. They are shown in Table 1.

We have also performed our own experiments in a new plasma reactor in order to determine recombination coefficients of various fusion relevant materials such as graphite and tungsten. Plasma was created by means of a radio frequency generator in a mixture of argon and hydrogen at pressure around 100 Pa. The degree of dissociation of hydrogen molecules was found to be between 0.1 and 1. Hydrogen atom density was measured by means of Fiber Optic Catalytic Probe. The recombination coefficient was determined by measuring axial profile of hydrogen atom density (Figure 3) and using Smith's side arm diffusion model. Recombination coefficients were found to vary with material and surface structure. Our results are listed in Table 2.

Table 1: Surface recombination of hydrogen

Material	Coefficient	Temp (K)	Pressure (Pa)	Method
Ag	0.13	298	0.26	Smith diffusion method
AISI 304	0.10	300		
Al	$10^{-3}$	298	0.26	Smith diffusion method
Al	0.29	328		catalytic probe
Al	0.32	328		catalytic probe
Al	0.21	423		catalytic probe
Al	0.27	733		catalytic probe
Al <sub>2</sub> O <sub>3</sub>	$0.90 \times 10^{-1}$	288		Smith diffusion method
Au	0.10	298	0.26	Smith diffusion method
Co	0.18	298	0.26	Smith diffusion method
Cr	0.16	298	0.26	Smith diffusion method
Cu	0.19	298	0.26	Smith diffusion method
Cu	0.14	333		catalytic probe
Cu	0.10	543		catalytic probe
Cu	0.10	693		catalytic probe
Fe	0.17	298	0.26	Smith diffusion method
fused silica	$0.23 \times 10^{-2}$ - $0.21 \times 10^{-3}$		130-650	Pulsed plasma excitation technique
glass	$0.18 \times 10^{-2}$	573		Smith diffusion method
hydrocarbons	$0.70 \times 10^{-1}$	400	177-3540	VUVAS-vac. ultraviolet absorb. spectr.
hydrogenated amorphous Si	$0.40 \pm 0.10$	350	40	TIMS-treshold ionisation mass spectrum.
Mn	0.20	298	0.26	Smith diffusion method
Ni	0.18	298	0.26	Smith diffusion method
Ni	0.25	303		catalytic probe
Ni	0.13	358		catalytic probe
Ni	0.20	423		EPR (electron paramagnetic resonance spectr.) and calorimetric technique
Ni	0.19	473		catalytic probe
Ni	0.17	623		catalytic probe
Ni	0.14	873		catalytic probe
Pd	0.20	298	0.26	Smith diffusion method
Pd	$0.80 \times 10^{-1}$	448		catalytic probe
Pd	$0.73 \times 10^{-1}$	448		catalytic probe
Pd	$0.52 \times 10^{-1}$	673		catalytic probe
Pd	$0.86 \times 10^{-1}$	763		catalytic probe
Pt	0.25	298	0.26	Smith diffusion method
Pt	$0.40 \times 10^{-1}$	376		EPR and calorimetric technique
Pt	$0.40 \times 10^{-1}$	378		EPR and calorimetric technique

Material	Coefficient	Temp (K)	Pressure (Pa)	Method
Pt	0.79 x 10 <sup>-1</sup>	588		EPR and calorimetric technique
Pt	0.10	813		EPR and calorimetric technique
Pyrex	0.75 x 10 <sup>-3</sup>	298	0.26	Smith diffusion method
Quartz	0.07 x 10 <sup>-3</sup>	288		Smith diffusion method
Quartz	0.26 x 10 <sup>-2</sup>	573		Smith diffusion method
Quartz	0.34 x 10 <sup>-2</sup>	773		Smith diffusion method
silica	0.50 x 10 <sup>-5</sup>	194		
silica	0.11 x 10 <sup>-2</sup>	920		
silica	0.86 x 10 <sup>-3</sup>	920		
silica	0.11 x 10 <sup>-2</sup>	980		
silica	0.15 x 10 <sup>-2</sup>	1140		
silica	0.36 x 10 <sup>-2</sup>	1240		
silica	0.33 x 10 <sup>-2</sup>	1240		
SiO <sub>2</sub>	0.18 x 10 <sup>-1</sup>	350	40	TIMS
Stainless steel	0.20	350	40	TIMS
Stainless steel	0.15	400	177-3540	VUVAS-vac. ultraviolet absorb. spectr.
Ti	0.100	298	0.26	Smith diffusion method
Ti	0.35	308		catalytic probe
Ti	0.40	308		catalytic probe
Ti	0.48	335		catalytic probe
Ti	0.35	421		catalytic probe
Ti	0.35	558		catalytic probe
V	0.15	298	0.26	Smith diffusion method
W	0.70 x 10 <sup>-1</sup>			Raynolds difussion coefficient
W	0.65 x 10 <sup>-1</sup>	353		catalytic probe
W	0.55 x 10 <sup>-1</sup>	423		catalytic probe
W	0.70 const.	443		EPR and calorimetric technique
W	0.70 const.	480		EPR and calorimetric technique
W	0.68 x 10 <sup>-1</sup>	533		catalytic probe
W	0.62 x 10 <sup>-1</sup>	563		catalytic probe
W	0.55 x 10 <sup>-1</sup>	573		catalytic probe
W	0.54 x 10 <sup>-1</sup>	578		catalytic probe
W	0.59 x 10 <sup>-1</sup>	643		catalytic probe
W	0.62 x 10 <sup>-1</sup>	678		catalytic probe
W	0.57 x 10 <sup>-1</sup>	723		catalytic probe
W	0.70 const.	773		EPR and calorimetric technique
W	0.62 x 10 <sup>-1</sup>	923		catalytic probe
W	0.67 x 10 <sup>-1</sup>	1088		catalytic probe

Table 2. Values of recombination coefficients determined by analyzing the axial hydrogen radical density profiles. An example of this profile is shown in Figure 3.

Material	Recombination coefficient	Standard deviation
85250 borosilicate glass	0.0032	0.0011
Tungsten	0.0025	0.0011
Carbon	0.0043	0.0018
Teflon	$< 10^{-3}$	

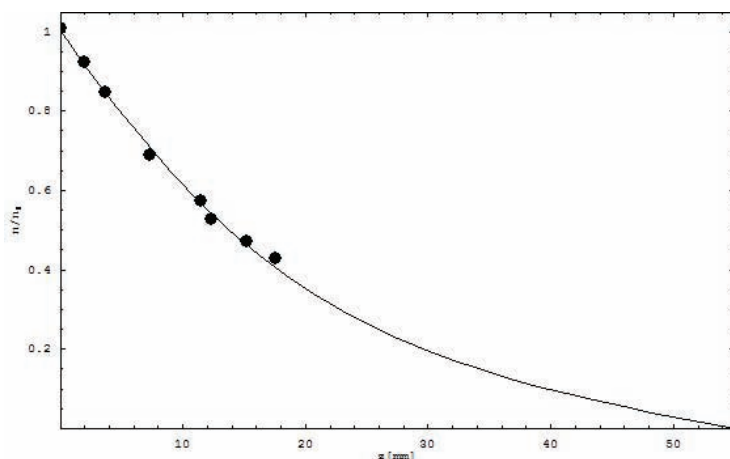


Figure 3. Axial hydrogen radical density profile for tungsten.

The experimental results were reported at the Plasma Conference in Tarragona, Spain (2 posters), and the Nuclear Conference in Bled, Slovenia (1 oral and 1 poster). We also attended the 1st Workshop of PCJ and IJS co-workers in Juelich, Germany, where we presented activities and planned future collaboration.

### 3 CONCLUSIONS AND OUTLOOK FOR 2006

The catalytic probes for H measurement have been used for characterization of our plasma reactor. In spring 2006 the probes will be adopted for measuring the H density in TEXTOR. Preliminary experiments are scheduled for June 2006. Experiments will be first performed in the simple DC glow discharge at the power of up to 7kW in order to test the compatibility with current TEXTOR facilities. Also in June 2006, first experiments in hot tokamak plasma will be performed at probe position a few cm below the plasma edge. The experimental results will be analyzed at our labs during the summer 2006. Further experiments will be performed in October/November 2006 at TEXTOR as parasitic users in order to test the probe in various tokamak plasmas. A researcher from our group will spend 4-5 weeks at TEXTOR to collect and analyse the data obtained by the probe.

Experimental work at the European solar facility in Font Romeu, France, is foreseen for late autumn 2006. Preliminary study of surface effects on fusion relevant materials during

exposure of materials to hydrogen plasma will be performed. The following materials will be used: carbon, tungsten and molybdenum. The materials will be exposed to a large flux of H atoms (between 1022 and 1024 atoms/(m<sup>-2</sup>s<sup>-1</sup>). The recombination rate of hydrogen atoms will be determined.

A visit to the Laboratorio Nacional de Fusion, As. Euratom/Ciemat, Av. Complutense 22, Madrid, 28040, Spain is foreseen for the last quarter of 2006. We will learn about particular characteristics of the plasma device and try to prepare probes suitable for application in Madrid.

## PUBLICATIONS

### Original articles

- [1] CVELBAR, Uroš, MOZETIČ, Miran, POBERAJ, Igor, BABIČ, Dušan, RICARD, Andre. Characterization of hydrogen plasma with a fiber optics catalytic probe. *Thin solid films.*, 2005, 475, pp. 12-16.
- [2] MOZETIČ, Miran, CVELBAR, Uroš, VESEL, Alenka, RICARD, Andre, BABIČ, Dušan, POBERAJ, Igor. A diagnostic method for real-time measurements of the density of nitrogen atoms in the postglow of an Ar-N<sub>2</sub> discharge using a catalytic probe. *J. appl. physi.*, 2005, vol. 97, pp. 103308-1-103308-7.

### Invited conference papers

- [3] MOZETIČ, Miran. Characterization of reactive plasmas with catalytic probes : presented at 5th Asian-European International Conference on Plasma Surface Engineering, (AEPSE'2005), 12-16 September, Qingdao City, China. 2005.

### Conference papers

- [4] MOZETIČ, Miran, VESEL, Alenka, EVANGELAKIS, Giorgos A. Determination of H density in a remote part of a hydrogen plasma reactor. V: *32nd EPS Conference on Plasma Physics [and] 8th International Workshop on Fast Ignition of Fusion Targets : programme : Tarragona, 27th June - 1st July 2005*. [S.l.: s.n.], 2005.
- [5] VESEL, Alenka, MOZETIČ, Miran, ZALAR, Anton. Interaction between neutral hydrogen atoms and weakly oxidized stainless steel surface. V: *32nd EPS Conference on Plasma Physics [and] 8th International Workshop on Fast Ignition of Fusion Targets : programme : Tarragona, 27th June - 1st July 2005*. [S.l.: s.n.], 2005.
- [6] MOZETIČ, Miran, VESEL, Alenka. Density of neutral hydrogen atoms in a microwave hydrogen plasma reactor. V: *International Conference Nuclear Energy for New Europe 2005, Bled, Slovenia, September 5-8. Book of abstracts*. [Ljubljana: Nuclear Society of Slovenia], 2005, str. 15.
- [7] VESEL, Alenka, MOZETIČ, Miran. Heterogeneous recombination of neutral hydrogen atoms on surfaces of the fusion relevant materials. V: *International Conference Nuclear*

Energy for New Europe 2005, Bled, Slovenia, September 5-8. *Book of abstracts.* [Ljubljana: Nuclear Society of Slovenia], 2005, str. 15.

[8] MOZETIČ, Miran, VESEL, Alenka. Heterogena rekombinacija nevtralnih vodikovih atomov na površinah materialov v fizijskih plazemskih reaktorjih. V: RADIĆ, Nikola (ur.). Vakumska znanost i tehnika - 12. Međunarodni sastanak, Trakošćan, 18. maja 2005. *Zbornik sažetaka.* Zagreb: Hrvatsko vakuumsko društvo, 2005, str. 31.

## Analysis of Narrow Support Element of The W7-X Magnet System under Design Loads

**Prof. Jože Duhovnik, Jerman B., Kolšek T., Kramar J., Mole N., Resman F., Štok B.**  
 University of Ljubljana,  
 Faculty of Mechanical Engineering,  
 Departments LECAD, LNMS, LASOK  
 Jozef.Duhovnik@lecad.uni-lj.si

### 1 INTRODUCTION

The magnet system of the Wendelstein 7-X (W7-X) stellarator device includes 50 non-planar and 20 planar coils (see Fig. 1). They are toroidally arranged in 5 identical periods, and antisymmetrically within each period. The weight of the coils and the electromagnetic loads occurring during operation are taken by a central support ring. The loads from each coil are transferred to the support ring via two central connection elements and to the neighbouring coils through lateral, contact, planar and narrow support elements. Narrow supports (NS) are one of the most critical components of the structure due to extremely high loads to be transmitted with simultaneous relative sliding and tilting between the coils, requirements for the cycle sliding without stick-slip effect and inaccessibility for checking/replacement (See Fig. 2).

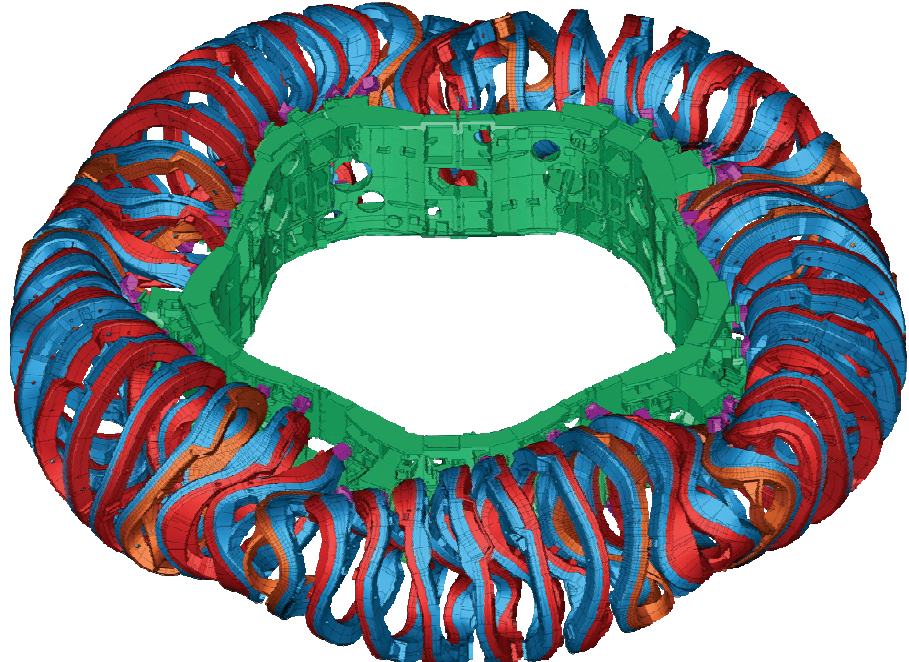


Figure 1: The geometry of the Wendelstein stellarator W7-X, 3D coil system

Global Finite Element (FE) analyses have been performed in the past primarily for the purpose of understanding the structural behaviour of whole magnet system, while preliminary local analysis has been carried out separately. IPP Greifswald (IPPG) requested a Finite element analysis of a Narrow Support Element NSE 1e7-2e4 of the Wendelstein stellarator

W7-X coil system and provided all necessary data in the form of 3D STEP format models, 2D drawings and tabular material data.

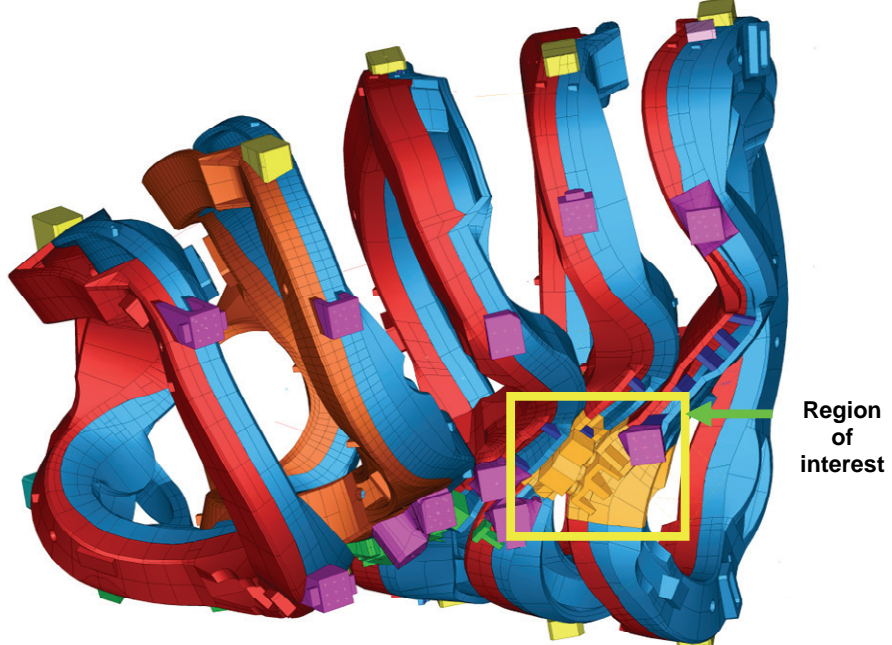


Figure 2: The »Half-Module« of the coil system, where the region of interest, the NSE connection, is indicated

The analysis assumed the load forces to cause the plastic deformation of the materials. Therefore, the material stress-strain characteristics for all relevant materials had to be taken into account. Additionally, the NSE connections are subject to operate at very low temperatures of 4K. A highly nonlinear elastic-plastic contact analysis had to be performed in order to obtain realistic results.

## 2 WORK PERFORMED IN 2005

A finite element analysis of the selected NSE type has been performed simultaneously with two popular engineering tools, ANSYS and ABAQUS. The aim was to obtain the load-deformation characteristics of the NSE connection in various directions and under various sliding conditions. The potential damage to the components at a chosen force level should be indicated. In the following, the analysis and the results are briefly reported.

### 2.1 Geometry

IPP requested a local analysis of the NSE connection and therefore supplied only a portion of the relevant geometry, i.e. part of the touching coils and the NSE components pad, and the pad frame. Since the target deformation of the system had been prescribed, we selected only a portion of the geometry to perform the detailed analysis, as shown on Figure 3.

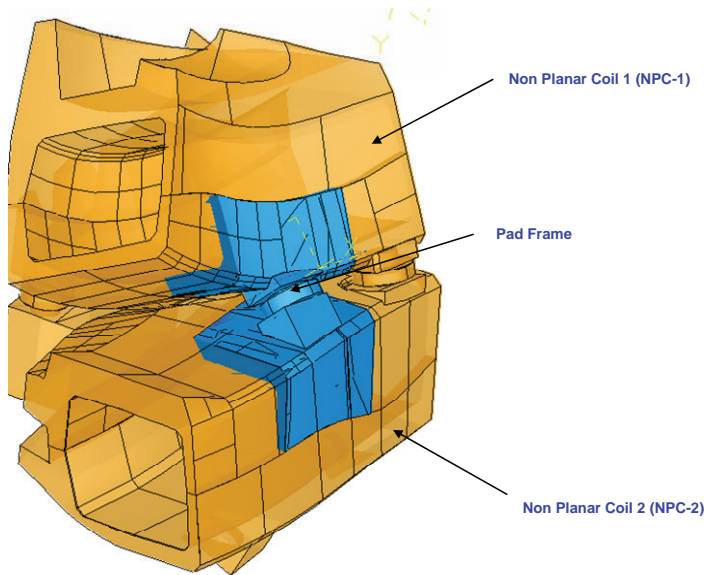


Figure 3: The geometry of the NSE and part of the coil casings; orange color: The geometry provided by IPPG, blue coding: the geometry entering analysis

The cross section of the relevant geometry is depicted on Figure 4.

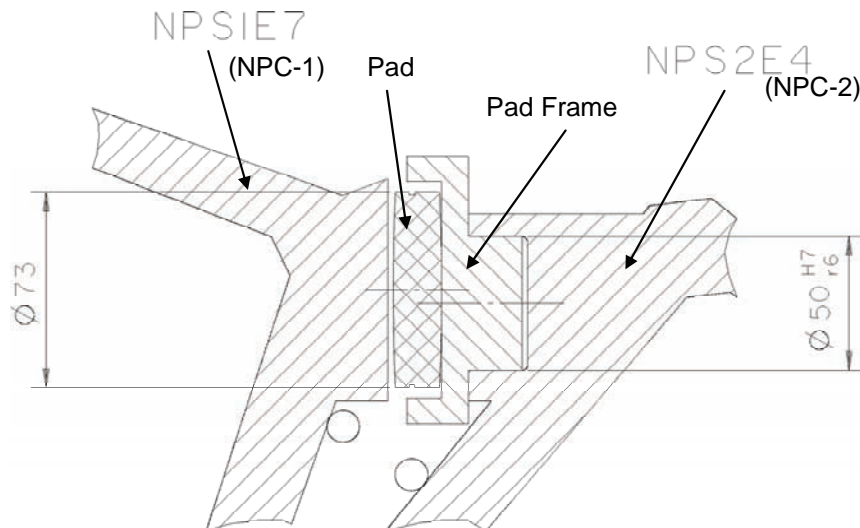


Figure 4: The cross section of the relevant geometry

The main parameters of the analysis to follow are:

a) the materials of the components:

Pad material – soft bronze alloy (AlBr1.0966)

Coil material -1.3960 steel

Frame material – 1.4429 steel

b) the geometry of the Pad: Pad diameter is 73 mm and the Pad curvature on both sides is 1100 mm

c) The compression force on the assembly is up to 3 MN

d) The analysis should involve cases with relative lateral shift of the coils up to 2 mm

- e) The friction between the components can vary in the range 0.1-0.3
- f) the shrink fit between NPC-2/PadFrame 0.05 mm overlapping should be taken into account, the initial gap between PadFrameCollar/NPC-2 is 0.03 mm
- g) The tilting of the surfaces in contact NPC-1/PadFrame should be up to 0.5 degree.

## 2.2 Material data

The analysis assumed the load forces to cause plastic deformation of the materials. Therefore, the material stress-strain characteristics for all relevant materials had to be taken into account. IPPG has provided necessary data in a tabular form. The stress-strain characteristics of all materials were highly nonlinear and temperature dependent.

## 2.3 Boundary conditions of the model

Since the model has been cut out of the whole non-planar coil system, we have agreed to use simplified boundary conditions at the cut surfaces. IPPG requested calculations of 6 distinctive computational cases, which differ by the initial pad position, application of shear force, application of the NC1 contact surface tilting and friction coefficient values (see Fig. 5).

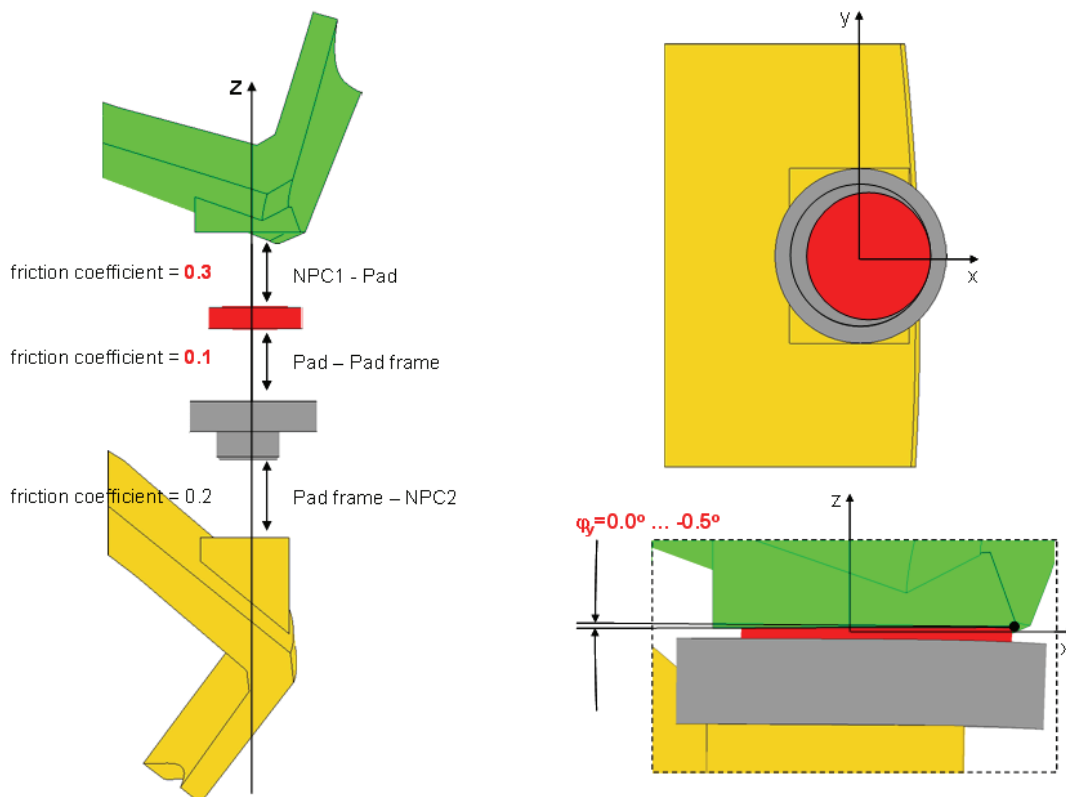


Figure 5: Parts in contact, position of the pad, and tilting

BC Case 1: a) An initial Pad position is at the maximum possible positive x-position with the respect to the Pad Frame, as shown on Fig 5; b) The initial tilt of the part NPC-1 is 0 degree and is gradually increasing in parallel to the compression force, until it reaches its maximum

value of 0.5 degree, the final state shown on Fig 5; c) A gradually increasing displacement of NPC-1 in +x direction is applied in parallel to the compression force, until it reaches its maximum value of 2 mm; as a result, shear force Fx force is computed; d) Friction coefficient Pad/Pad frame is 0.1 and Friction coefficient for Pad/NPC-1 is 0.3, see Fig 5;

BC Case 2: a) An initial Pad position is at the center; b) No tilt of the part NPC-1 is applied; c) No shear force is applied; d) Friction coefficient Pad/Pad frame is 0.2 and Friction coefficient for Pad/NPC-1 is 0.2;

BC Case 3: a) An initial Pad position is at the center; b) No tilt of the part NPC-1 is applied; c) A gradually increasing shear force Fx is applied in parallel to the compression force in +x direction; d) Friction coefficient Pad/Pad frame is 0.2 and Friction coefficient for Pad/NPC-1 is 0.2;

BC Case 4: a) An initial Pad position is at the center; b) No tilt of the part NPC-1 is applied; c) A gradually increasing shear force Fx is applied in parallel to the compression force in -x direction; d) Friction coefficient Pad/Pad frame is 0.2 and Friction coefficient for Pad/NPC-1 is 0.2;

BC Case 5: a) An initial Pad position is at the center; b) No tilt of the part NPC-1 is applied; c) A gradually increasing shear force Fy is applied in parallel to the compression force in +y direction; d) Friction coefficient Pad/Pad frame is 0.2 and Friction coefficient for Pad/NPC-1 is 0.2;

BC Case 6: a) An initial Pad position is at the center; b) No tilt of the part NPC-1 is applied; c) A gradually increasing shear force Fy is applied in parallel to the compression force in -y direction; d) Friction coefficient Pad/Pad frame is 0.2 and Friction coefficient for Pad/NPC-1 is 0.2;

We have run an initial BC Case 1 case by gradually increasing the displacement of the NPC-2 in +normal-direction until the reaction force at the cutter surfaces in normal-direction was 3.0 MN. The maximum value of the NPC-2 displacement in normal-direction was 2.56 mm. An initial overlapping between the Pad frame and NPC-2 of 0.05 mm was taken into account. The component's contact has been modelled by surface to surface contact elements, which were attached to all nodes, which could possibly be in contact. The contact has been established between the following surfaces: NPC1-Pad, Pad-PadFrame, Pad frame-NPC2 (see Figure 5).

### 3 RESULTS

There were numerous results providing insight into the behaviour of individual NSE components under design loads. A report comprising more than 100 pages including details has been submitted to IPPG. Only a small selection is provided here. Figures 6 and 7 show the equivalent plastic strain of the components in contact, which indicate severe plastic deformation both in pad and pad frame.

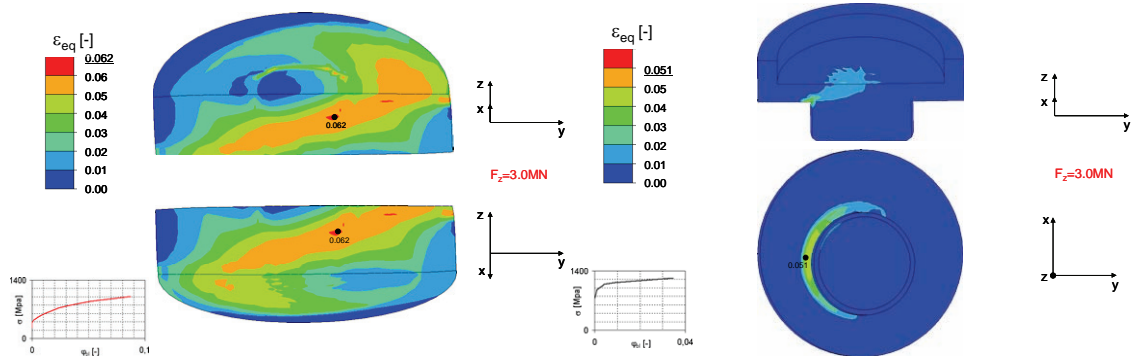


Figure 6: Equivalent plastic strain at the PAD, and Pad Frame,  $F=3.0 \text{ MN}$

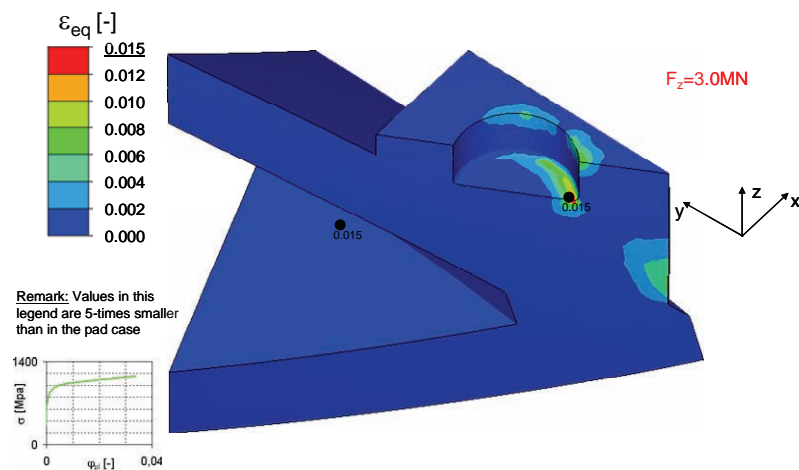


Figure 7: Equivalent plastic strain at the NPC-2,  $F=3.0 \text{ MN}$

As the main result, the characteristic stiffness curves in multiple directions have been calculated (see example on Fig. 8). There were some small differences observed between ANSYS and ABAQUS results.

The difference between individual points on stiffness curves in all cases were relatively small, in the vast majority of the points less than 10%. Both tools yielded curves of the same characteristic nonlinear shape. There were substantial differences in shear-stiffness characteristics in BC Cases 3, 4, 5 and 6 (see example on Fig 9). It turned out, that these cases were handled with different boundary conditions as follows: ABAQUS analysis used the following BC3: A gradually increasing shear force  $F_x$  has been applied in parallel to the compression force in  $+x$  direction as a consequence of the prescribed movement of the boundary faces of the coil casing, until it reached 2mm in  $+x$  direction; Sliding has been prevented by increasing friction; A preliminary calculation has been performed to synchronize it with the vertical movement; ANSYS tool used the following BC3: A gradually increasing shear force  $F_x$  has been applied in parallel to the compression force in  $+x$  direction;  $F_x$  has been calculated as  $0.199 \cdot F_z$  to avoid sliding; A preliminary calculation has been performed to synchronize it with the vertical compression force; The analogous application of BC was performed for BC4, BC5, BC6;

The differences between the characteristics computed by ABAQUS and ANSYS are attributed to the differences in the vendor code handling the nonlinearities in terms of material behaviour, large deflections and contact problems.

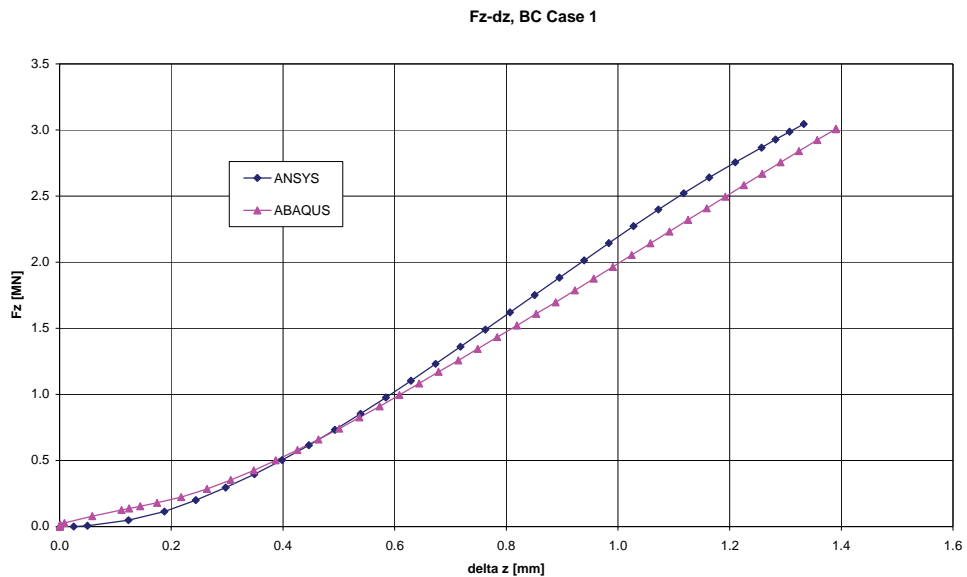


Figure 8: Compression force versus vertical displacement, BC Case 1

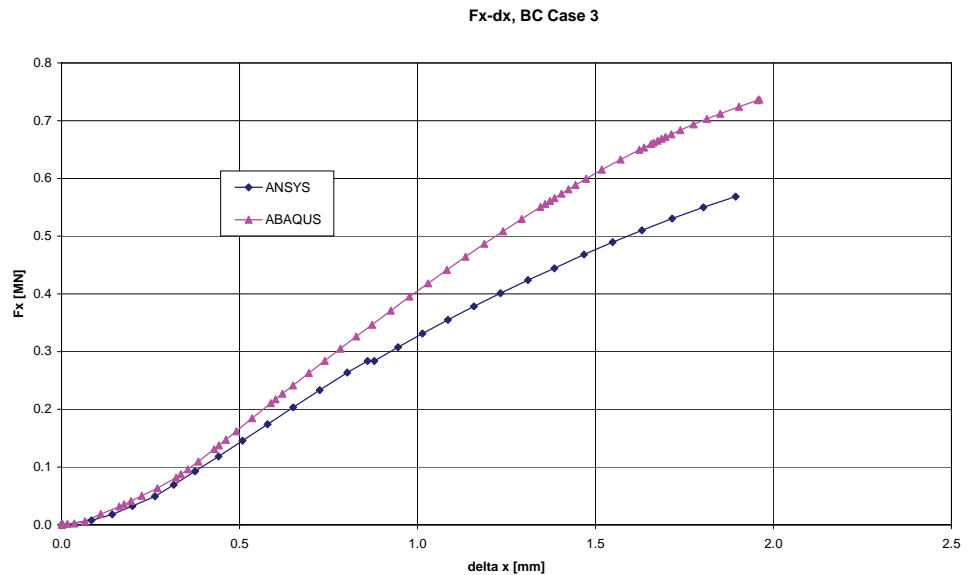


Figure 9: Shear force versus x-displacement, BC Case 3

#### 4 OUTLOOK FOR 2006

The successful completion of the project initiated further collaboration between IPP Greifswald and UNI-Ljubljana. A new 2006 project was defined to evaluate the design of six different NSE and to determine the limit and allowable forces during W7-X operation. Another project was defined in order to perform cyclic loading simulation.



## Application of Ion Beam Analytical Methods to the Studies of Plasma Wall Interaction in Tokamaks

**Primož Pelicon, Iztok Čadež, Zvone Grabnar, Darko Hanžel, Matjaž Kavčič,  
Zdravko Rupnik, Jure Simčič**

“Jožef Stefan” Institute,  
Department for Low and Medium Energy Physics  
Primož.Pelicon@jjs.si

### 1 INTRODUCTION

Plasma-wall interactions in controlled fusion devices largely influence the plasma properties. The interaction of the plasma with the plasma-facing components (PFCs) results in material erosion, transport and re-deposition. Plasma-wall interaction is currently studied in relation to the choice of materials for plasma facing components in ITER and also for the experiments on existing smaller tokamaks. These problems are related to the material erosion and deposition, gas balance, influence of transient heat loads to the wall, use of high Z plasma facing materials, and hydrogen retention and removal from the plasma wall.

Characterisation of materials before and after the exposure to the fusion plasma during well-characterised single experiments or after longer time is performed by numerous complementary methods. Among these methods Ion Beam Analysis (IBA) methods are often used as they give reliable absolute elemental and isotopic depth concentration profiles in the studied solid surfaces. Ex-situ analyses of such surfaces improve the understanding of processes responsible for erosion, re-deposition and in-vessel fuel retention.

#### 1.1 Castellated graphite limiter

The limiter consisted of seven molybdenum and one graphite castellated sections has been exposed under erosion-dominated conditions in the SOL of tokamak TEXTOR, Forshungszentrum Juelich. The aim of the analysis performed at JSI with high-energy focused proton beam was to determine the molybdenum distribution at the exposed surfaces as well as inside the castellation gaps of the limiter carbon section.

The macroscopic areal density profiles were measured with high-energy focused proton beam and high lateral resolution scans were made. At the macroscopic scale (fig. 1), it was evident that deposition has been increased in the centres of the castellated structures facing plasma and reduced at the regions closer to castellation gaps.

At the micrometer resolution (fig. 2) two regimes of the Mo deposition processes on graphite parts were observed. At the plasma exposed graphite surface, islands of the Mo material on graphite were formed with a peaked area density exceeding  $3 \times 10^{18}$  Mo at/cm<sup>2</sup> and characteristic lateral dimension of 20 – 50 µm. The plasma-exposed parts of the castellation gaps also have island-like deposits, whereas plasma-shadowed surfaces deeper in the gaps are covered with a continuous Mo-containing film.

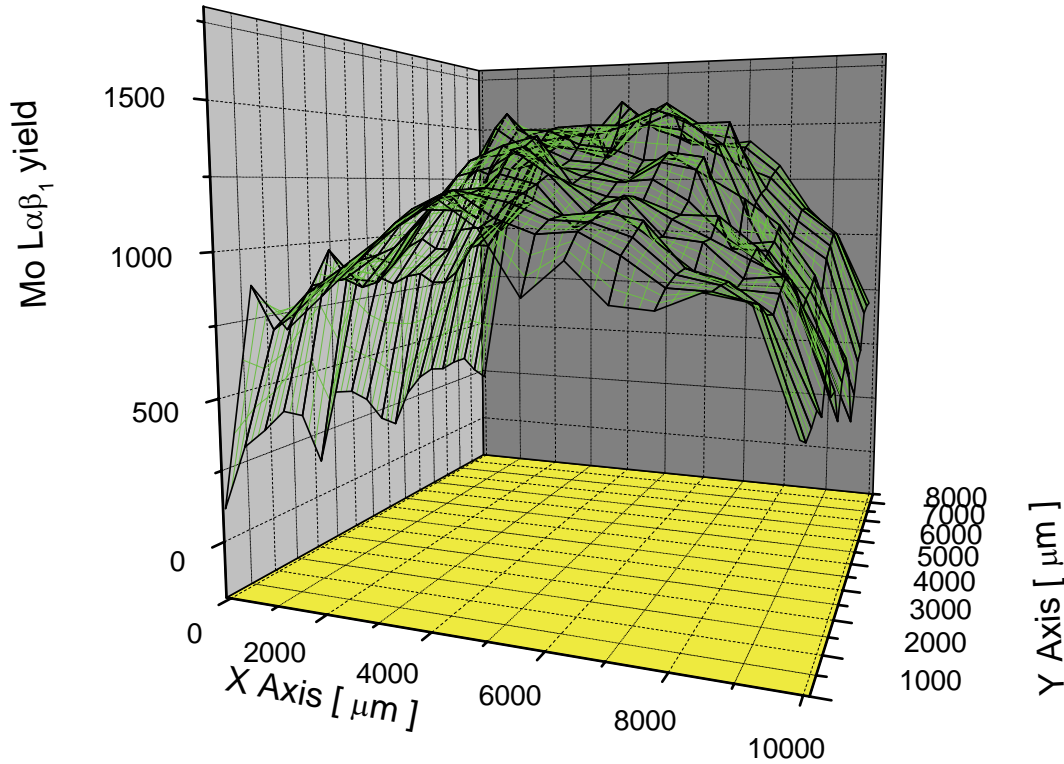


Figure 1: The molybdenum deposition pattern at the graphite section of the limiter over an area of  $10 \times 10 \text{ mm}^2$  at the sector 4 (see also fig.2). Areal density of re-deposited molybdenum is lower close to the castellation gap.

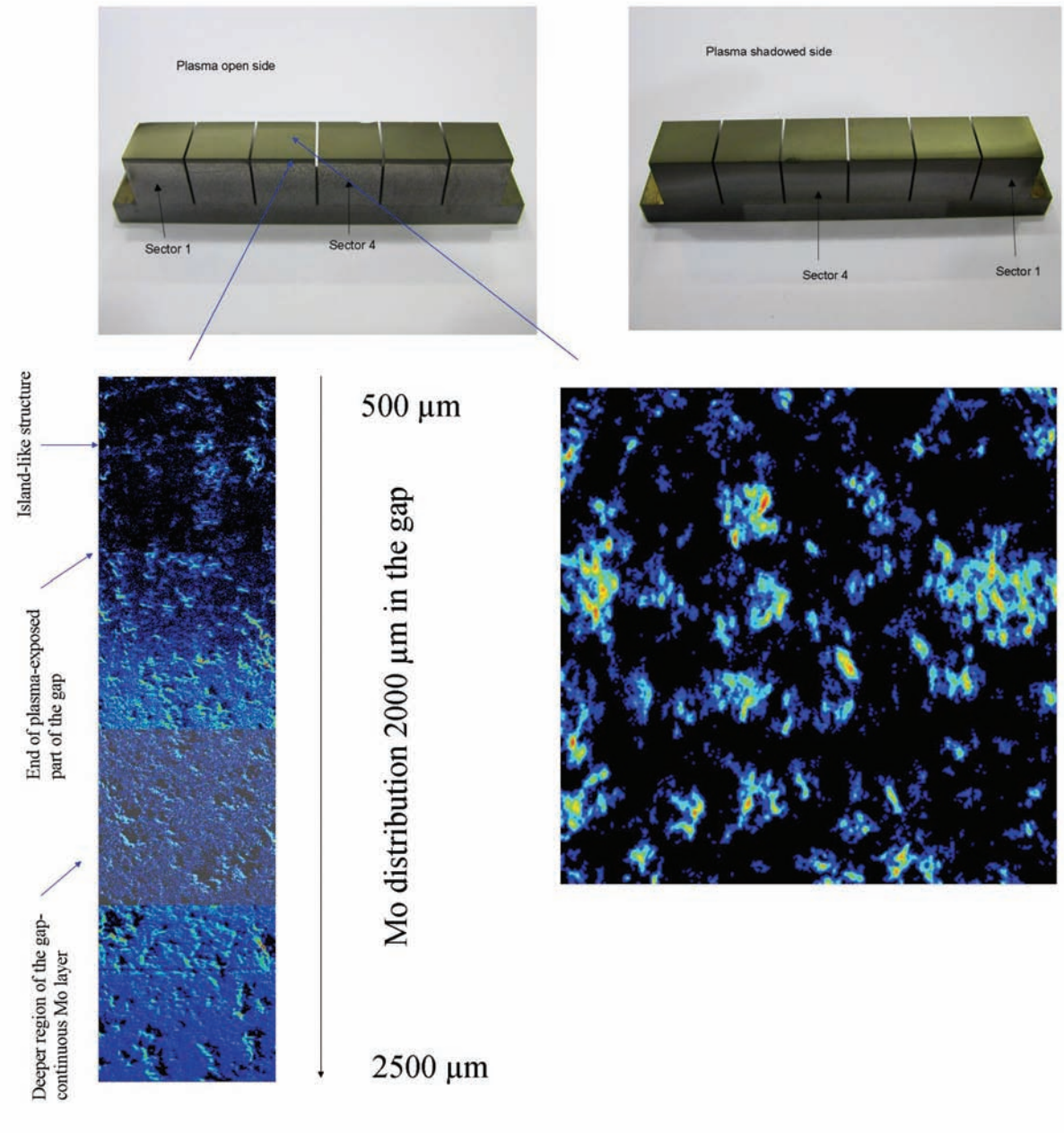


Figure 2: Lateral microdistribution of re-deposited molybdenum at the graphite section of hybrid Mo/C castellated structure after plasma exposure under erosion-dominated conditions in the SOL of tokamak TEXTOR. Island-like deposit structure is formed in the regions directly exposed to plasma. Deeper in the castellation gap the deposit is in the form of continuous layer.

## 1.2 Pump duct probes

The research on the field of pump duct probes, which reveal a long-term migration of the deposits inside the pump duct tubes of the TEXTOR, has been performed in collaboration with the group from Forschungszentrum Jülich, Association EURATOM-FZJ, to reveal deposition rates and the nature of the deposits. The exposed probes were removed from the pump ducts and shipped to JSI for the analysis of the H and D content in the deposited layer.

Elastic Recoil Detection Analysis [1] with 4.2 MeV  $^7\text{Li}$  was used to measure the H and D areal densities at several regions along the pump ducts in order to understand the mechanism of fuel retention and deposit formation (see Fig. 3).

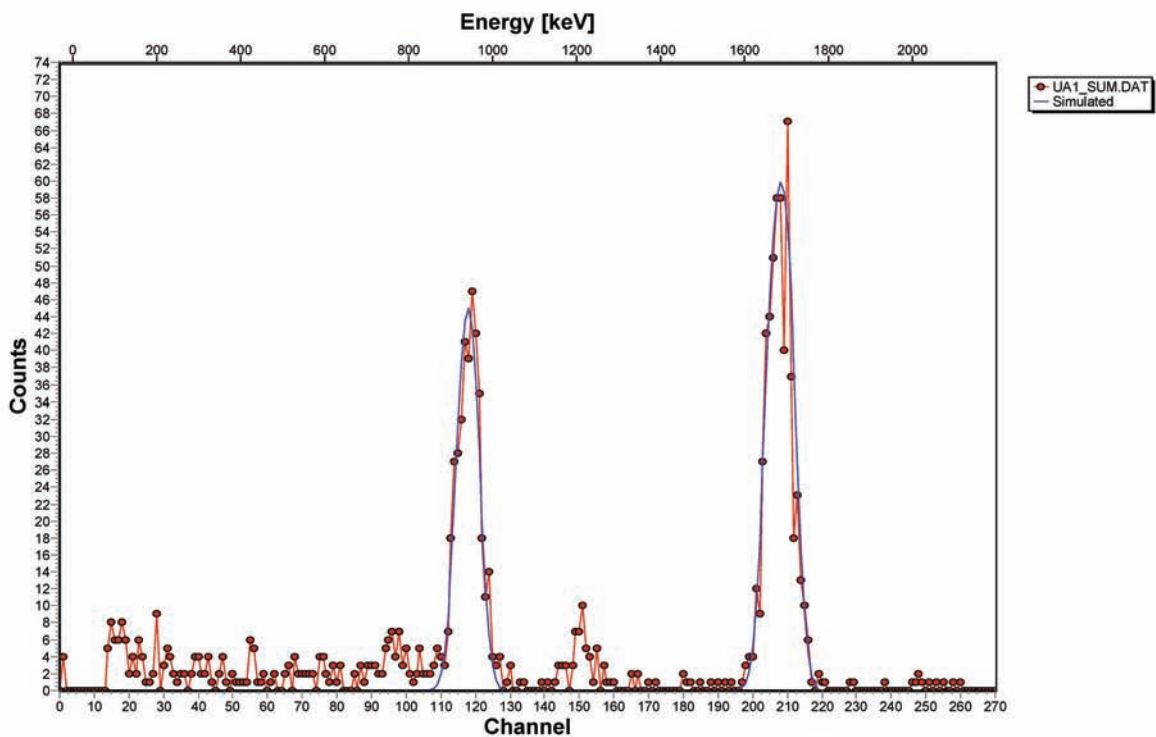


Figure 3: Elastic Recoil Detection Analysis spectrum measured at silicon pump duct probe from TEXTOR. Deuterium and hydrogen peak area is proportional to the surface area density of deuterium and hydrogen. Evaluation of the spectra is done with the SIMNRA code (M. Mayer, IPP Garching).

## 2 CONCLUSIONS AND OUTLOOK FOR 2006

In the year 2006, the work will be focused on the fuel retention in the plasma-exposed wall regions and gaps in castellation structures. Measurement method on microdistribution of hydrogen isotopes (isotope mapping) accumulated in the wall materials require both high lateral resolution of the method applied as well as isotopic mass resolution. The method of Elastic Recoil Detection Analysis with focused Li beam is a candidate fulfilling both demands and will be developed for isotope mapping in wall materials.

## PUBLICATIONS

### Original articles

- [1] PELICON, Primož, RAZPET, Alenka, MARKELJ, Sabina, ČADEŽ, Iztok, BUDNAR, Miloš. Elastic recoil detection analysis of hydrogen with  $^7\text{Li}$  ions using a polyimide foil as a thick hydrogen reference. *Nucl. instrum. meth. B*, 2005, vol. 227, p. 591-596.

### Conference abstracts

- [2] RAZPET, Alenka, ČADEŽ, Iztok, PELICON, Primož, MARKELJ, Sabina, BREZINŠEK, Sebastijan. ERDA analysis of hydrogen and deuterium in the plasma-exposed graphite surfaces from the tokamak TEXTOR. V: XVII International Conference on Ion Beam Analysis, IBA 2005: June 26- July 1, 2005, Seville, Spain, Book of abstracts, P-Tue-072.

- [3] Pelicon Primož, Čadež Iztok, Smarkelj Sabina, Simčič Jure, Rupnik Zdravko, Analysis of materials used for plasma-facing components in tokamaks with ion beam analytical techniques, International Conference “Nuclear Energy for New Europe 2005”, Book of Abstracts, page 16.



## Collaboration in DEMO Working Group

**Matjaž Ravnik**  
“Jožef Stefan” Institute  
Reactor Physics Department  
Matjaz.Ravnik@ijs.si

### 1 INTRODUCTION

The purpose of the project is to contribute and to make available to the DEMO Working Group the knowledge and the expertise on the conventional aspects of the DEMO power station as a nuclear installation. Main aspects of interest are: neutron transport and activation, technology of the secondary side, nuclear waste, licensing, safety analysis and emergency preparedness. In the conceptual design phase of the project which was the continuous task of the DEMO Working Group in 2005, the interest of the group was mainly in basic problems of fusion technology and less in the conventional aspects that are believed to be solved, at least to a much wider extent than other typical fusion problems. For this reason, my contribution was mainly on general aspects of radioactive waste treatment.

### 2 WORK PERFORMED IN 2005

The main task of the DEMO Working Group in 2005 was the conceptual study of the reactor and of the plant (1). An original document was upgraded and discussed at the meeting. My contribution was minor as the main problems were not in the conventional technology. I studied the materials focusing on conventional technology. I made some remarks and proposed small corrections that were considered by the DWG and some of them included in the study.

My main contribution was on the problem of the radioactive waste. During the discussion at a DWG meeting, the question of long lived radioactive waste was opened, in particular its disposal. It became evident that some long lived waste could be expected (although in limited amount), in particular if the reprocessing of the waste would be too expensive. It was concluded, that the disposal of long lived waste should be investigated, to be prepared for this option. I was asked to prepare a study on legal and technological aspects of radioactive waste treatment in Europe, including a review of existing and projected capacities. I presented the study at a DWG meeting (2).

The study included the following aspects:

- Classification of radioactive waste
- Technological solutions for storing and disposal
- Review of disposal programs in the EU and other countries
- Disposal programs in Sweden, France and Germany

The focus was on low and intermediate level radioactive waste. Regulations and relevant standard practice for fission reactor waste were considered. National and IAEA regulations were considered and compared. A detailed review of radioactive waste disposal practices was provided for Europe and the world.

The study and the presentation was discussed and accepted by the DWG. The general result of the discussion may be summarized as follows: It may be expected that some radioactive waste will have to be categorized as long-lived low or intermediate level radioactive waste, according to IAEA and national standards. However, technological solutions and capacities for their storing and disposal exist and will be available, as such capacities have to be provided for the waste from fission reactors. The problem of long-lived waste disposal from DEMO (and other fusion reactors) is marginal compared to waste disposal from fission reactors.

A world review of the repository options is provided in Table 1.

#### 1. Status of low and intermediate level waste disposal facilities in various countries

Country	Repository (date opened/closed)	Repository Concept
<b>In the process of site selection</b>		
Australia		ENSF
Belgium		ENSF
Brazil		ENSF
Bulgaria		ENSF
Canada (historic LLW)		-
China (East)		-
(Southwest)		-
Croatia		-
Cuba		MC
Ecuador		ENSF
Hungary		-
Indonesia		ENSF
Korea, Republic of		-
Pakistan		-
Slovenia		-
Turkey		ENSF
United Kingdom		GR
United States (Connecticut)		-
(Illinois)		ENSF
(Massachusetts)		-
(Ohio)		ENSF

(Michigan)		ENSF
(New Jersey)		-
(New York State)		ENSF
(Pennsylvania)		ENSF
<b>Site selected</b>		
China	Guangdong Daya Bay	ENSF
Cyprus	Ari Farm	SNSF
Egypt	Inshas	ENSF
Mexico	Laguna Verde	ENSF
Peru	RASCO	ENSF
Romania	Cernavoda	ENSF
Switzerland	Wellenberg	MC
<b>Under licensing</b>		
Canada	Chalk River	ENSF
Germany	Konrad	GR
Norway	Himdalen	MC
United States	Ward Valley, California	ENSF
	Boyd County, Nebraska	ENSF
	Wake County, North Carolina	ENSF
	Fackin Ranch, Texas	ENSF
<b>Under construction</b>		
China	Gobi, Gansa	ENSF
<b>In operation</b>		
Argentina	Ezeiza (1970-)	ENSF
Azerbaijan	Baku (1960s-)	ENSF
Australia	Mt. Walton East (1992-)	ENSF
Belarus <sup>1</sup>	Ekores, Minsk reg.(1964-)	ENSF
Brazil	Abadia de Goias (1996-)	ENSF
Czech Republic	Richard II (1964-)	MC
	Bratrstvi (1974-)	MC
	Dukovany (1994- )	ENSF
Slovak Republic	Mohovce (2001-)	ENSF
Finland	Olkiluoto (1992-) Loviisa (1997-)	MC
France	Centre de l'Aube (1992-)	ENSF
Germany	Morsleben (1981-)	GR
Georgia	Tbilisi (1960s-)	ENSF
Hungary	RHFT Pusokszilagy (1976-)	ENSF
India	Trombay (1954-)	S/ENSF
	Tarapur (1968-)	ENSF

	Rajasthan (1972-)	ENSF
	Kalpakkam (1974-)	ENSF
	Narora (1991-)	ENSF
	Kakrapar (1993-)	ENSF
Iran	Kavir Ghom-desert (1984-)	SNSF
Israel	Negev Desert	SNSF
Japan	Rokkasho (1992-)	ENSF
Kazakstan	Almaty	ENSF
	Kurchatov (1996-)	ENSF
	Ulba (1996-)	ENSF
Kyrgyzstan	Tschuj (1965-)	ENSF
Latvia	Baldone (1961-)	ENSF
Mexico	Maquixco (1972- )	SNSF
Moldova	Kishinev (1960-)	ENSF
Pakistan	Kanupp (1971-)	SNSF
	PINSTECH (1969-)	SNSF
Poland	Rozan (1961-)	ENSF
Romania	Baita-Bihor (1985-)	GR
Russia <sup>2</sup>	Sergiev Posad, Moscow reg. (1961-)	ENSF
	Sosnovyi Bor, Leningrad reg.	ENSF
	Kazan, Tatarstan	ENSF
	Volgograd	ENSF
	Nijnyi Novgorod	ENSF
	Irkutsk	ENSF
	Samara	ENSF
	Novosibirsk	ENSF
	Rostov	ENSF
	Saratov	ENSF
	Ekaterinburg	ENS
	Ufa, Bashkortostan	ENSF
	Cheliabinsk	ENSF
	Habarovsk	ENSF
South Africa	Pelindaba (1969-)	SNSF
	Vaalputs (1986-)	SNSF
Spain	El Cabril (1992-)	ENSF
Sweden	SFR (1988-)	MC
	Oskarshamn NPP (1986-)	SNSF

	Studsvik (1988-)	SNSF
	Forsmark NPP(1988-)	SNSF
	Ringhals NPP (1993-)	SNSF
United Kingdom	Dounreay (1957-)	SNSF
	Drigg (1959-)	S/ENSF
Ukraine	Dnepropetrovsk center	ENSF
	L'vov center	ENSF
	Odessa center	ENSF
	Kharkov center	ENSF
	Donetsk center	ENSF
United States	RWMC, INEEL (1952-)	S/ENSF
	SWSA 6, ORNL (1973-)	S/ENSF
	Disposal Area G, LANL (1957-)	SNSF
	Barnwell, South Carolina (1971-)	SNSF
	200 East Area Burial Ground, Hanford (1940s-	SNSF
	200 West Area Burial Ground, Hanford (1996-	SNSF
	Richland, Washington (1965-)	SNSF
	Savanah River Plant site (1953-)	SNSF
Uzbekistan	Tashkent (1960s-)	ENSF
Viet Nam	Dalat (1986-)	ENSF
<b>Operation stopped or under closure</b>		
Armenia	Erevan	ENSF
Bulgaria	Novi Han (1964-1994)	ENSF
Estonia	Tammiku (f. Saku) (1964-1996)	ENSF
France	Centre de la Manche (1969-1994)	ENSF
Germany	Asse (1967-1978)	GR
Russian Federation <sup>2</sup>	Murmansk	ENSF
	Groznyi, Chechnya	ENSF
Tajikistan	Beshkek	ENSF
Ukraine	Kiev center (-1992)	ENSF
<b>Closed</b>		
Czech Republic	Hostim (1953-1965)	MC
Hungary	Solymar (1960-1976) <sup>3</sup>	ENSF
Japan	JAERI, Tokai (1995-1996)	SNSF
Mexico	La Piedrera (1983-1984)	ENSF

Norway	Kjeller (1970-1970) <sup>4</sup>	ENSF
Lithuania	Maishiogala (1970s-1989)	ENSF
United States	Beatty, Nevada (1962-1992)	ENSF
	Maxey Flats, Kentucky (1963-1978)	SNSF
	ORNL SWSA 1 (1944-1944) <sup>3</sup>	SNSF
	ORNL SWSA 2 (1944- 1946)	SNSF
	Shefield, Illinois (1967-1978)	SNSF
	West Valley, New York (1963-1975)	SNSF

### Notes on the table

*Abbreviations:* SNSF = Simple Near Surface Facility MC = Mined Cavity ENSF = Engineered Near Surface Facility GR = Geological Repository S/ENSF = SNSF and ENSF

<sup>1</sup> There are 77 repositories built to accommodate waste from the Chernobyl accident.

<sup>2</sup> Repositories in the Russian Federation started operation from 1961 to 1967.

<sup>3</sup> Waste was moved to another repository (respectively, from Solymar to RHFT Pusokszilagy; and from ORNL SWSA-1 to ORNL SWSA-2).

<sup>4</sup> Waste will be moved to a new repository (Himdal) when constructed.

(1)

## 3 CONCLUSIONS AND OUTLOOK FOR 2006

In 2006 the work continues according to the STAC guidelines and the DWG program. The goal of this project (P-7) remains the same.

## PUBLICATIONS

(1) A CONCEPTUAL STUDY OF COMMERCIAL FUSION POWER PLANTS,  
Final Report of the European Fusion Power Plant Conceptual Study (PPCS), April 13, 2005  
EFDA-RP-RE-5.0

(2) M. Ravnik, Radioactive Waste Storing and Disposal in European Countries. Presentation at the DWG Meeting, Garching, 14 September 2005.

## Gas impermeable Coating for SiC<sub>f</sub>/SiC

S. Novak, G. Dražić, K. Mejak, N. Drnovšek, T. Toplišek, T. Žagar\*

“Jožef Stefan” Institute  
Department for Nanostructured Materials  
\*Department for Reactor Physics  
Sasa.Novak@ijs.si, Goran.Drazic@ijs.si

### 1 INTRODUCTION

The aim of this work was to improve the particular properties of the SiC<sub>f</sub>/SiC composite, prepared by CVI technology. As one of the drawbacks of the CVI material are connected to residual open porosity, the objective within this task was to coat the composite by a dense layer of the SiC-based material having properties adequate for use in a fusion reactor. The main problem to be solved to achieve this goal is linked to high temperatures and pressure needed for the sintering of the covalent SiC. For this reason we have been focused in determining a suitable coating material, which can be applied on the surface of the SiC/SiC and sintered at acceptable conditions to close-to-zero porosity. Throughout the project, the specific requirements of materials for fusion applications, especially the need to ensure minimum activation after n-irradiation, were taken into account.

### 2 WORK PERFORMED IN 2005

The key task in production of a dense SiC-coating is densification at temperatures, where no detrimental effect on the substrate material appears. Due to the covalent nature of the SiC, this is only possible by transient liquid-phase sintering, which is, however, usually performed at temperatures close to 2000°C. Additionally, full densification must be achieved by using only low activation additives and the dimensional changes have to be close to zero in order to avoid defects formation in the coating. Hence, the specific needs for the material require a thorough investigation of the densification of the coating material.

#### 2.1 Low-temperature densification of low-activation SiC-materials for the coating

Based on the available phase diagrams, we selected and have systematically investigated several possible compositions of the binder phase for SiC, based on the system SiO<sub>2</sub>-Al<sub>2</sub>O<sub>3</sub>-P<sub>2</sub>O<sub>5</sub> that produces a transient liquid phase at temperatures below 1500°C. Within the study of material's densification, the samples with various compositions containing micron-sized or nano-sized SiC powder and the additives were prepared by homogenization in aqueous suspensions. Special care was taken to minimize oxidation of the powder during processing.

First we prepared the samples of the material for the coating by homogenization of aqueous suspensions of SiC powder with the additives, followed by drying and dry pressing or slip-casting in non-porous mold. The disc-shaped samples with diameter of 6 mm were then fired in inert atmosphere at temperatures in the range of 1300 to 1500°C. Microstructures were observed by optical microscopy, SEM, FESEM and TEM. In particular the porosity was estimated.

## 2.2 Production of gas-impermeable ceramic coatings on SiC(f)/SiC

Coating of the samples of SiC/SiC(CVI) composite with the SiC-based material was performed by simple immersion of the substrate in the ceramic slurry, or alternatively, electrophoretic deposition (EPD) was tested. In the first case, we used aqueous suspensions in which we immersed surface modified sample of SiC/SiC for a few seconds to collect the coating material on its surface. After slow drying in humid atmosphere, the coated samples were fired at 1300 to 1500°C. The samples were cut perpendicular to the coating and polished, Fig. 1.

The preliminary experiments with electrophoretic deposition of the coating material revealed that the aqueous suspensions are not suitable for the deposition due to the electrolysis of water and consequently the formation of bubbles. The deposit, that was first formed on steel substrates, was either porous or even did not adhere to the substrate. Further experiments performed with ethanol suspension of the submicron-sized SiC powder without additives confirmed the feasibility of the method. Within ten minutes, a thick deposit was formed at the steel electrode or at the SiC/SiC bar used as an electrode, as illustrated in Figure 2. The technique obviously enables a fast deposition of the coating on the SiC/SiC composite.

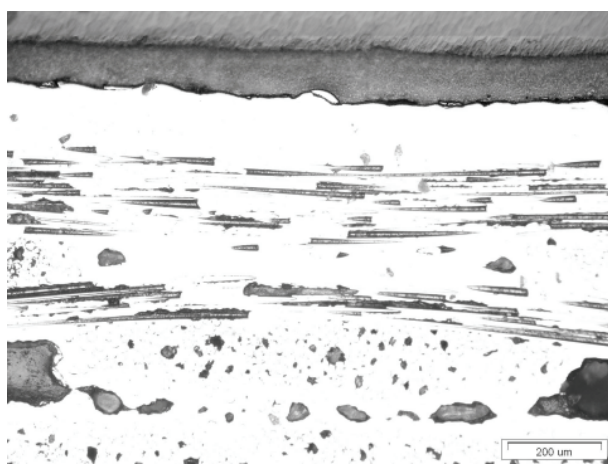


Fig. 1: Optical micrograph of the coating on the SiC/SiC(CVI) sample

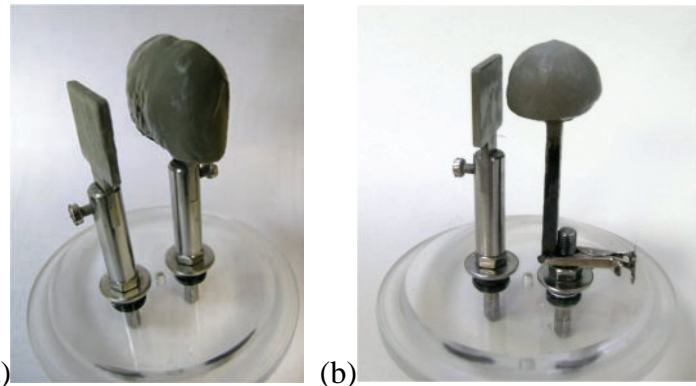


Fig. 2: Thick SiC deposits on (a) steel electrode and (b) on SiC/SiC(CVI) bar, formed in 10 minutes, illustrating the applicability of the electrophoretic deposition technique for the coating.

The addition of the sintering additives to ethanol-based SiC suspension for the deposition revealed certain colloidal incompatibility, suggesting that a thorough analysis of the electrokinetic properties will be needed in continuation. Preliminary trial-and-error experiments with deposition on a bundle of SiC fibres resulted in a deposit, rather well attached at the fibres, however, a thorough analysis of the microstructure after sintering revealed a need to improve processing conditions in particular focused on avoiding the oxygen.

The EPD was less successful with nano-sized particles, that is probably connected with the very low surface charge at the nano-sized particles. The analysis of the powders surface and adequate surface modification is therefore proposed for the next stage.

### 2.3 TEM characterization of coatings

The TEM micrograph of the SiC-matric material for the coating with nano-SiC powder is shown in Figure 3. It is evident that after sintering at 1300°C the SiC particles size remain nearly unchanged, suggesting that only rearrangement took place during firing. As presented, the secondary glassy phase (S) between particles (SiC) contains a certain amount of oxygen, presumably resulting from the oxygen containing surface layer at the particles. In further work the amount and the thickness of the secondary phase will be decreased.

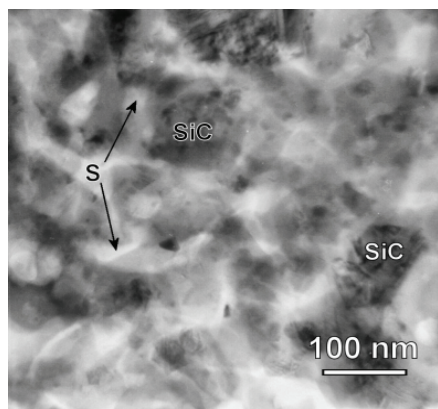


Figure 3: TEM micrograph of the SiC-based coating material, showing dark nano-sized SiC particles and the  $\text{Al}_2\text{O}_3$ - $\text{P}_2\text{O}_5$ - $\text{SiO}_2$  secondary phase (S)

## 2.4 Physical characterization of coating material and coated SiC(f)/SiC

**XRD:** In the sintered samples with submicron and nano-SiC powders the main phase is SiC and a certain amount of SiO<sub>2</sub> is also evident, while due to their low amount in the secondary phase of the sintered materials, no aluminium and phosphorus are detected. As expected, the amount of SiO<sub>2</sub> in the sample with nano-SiC is higher than for the submicron-SiC sample.

**Microhardness** of the coating materials with different compositions and sintered at various conditions was analysed by a Fischeroscope analyzer at the maximum load of 1000 N. The results are presented in Table 1 and in Figure 4.

Table 1:

Sample Id.	D <sub>SiC</sub> (μm)	Starting composition	Sintering T (°C)	Sintering time (hours)	μHV (GPa)
98	0.5	SiC / 39 B*	1300	<u>2h</u>	349
99	0.5	SiC / 39 B	<u>1450</u>	3h	250
100	0.5	SiC / 39 B	1300	3h	303
102	0.5	SiC / 39 B	1300	<u>4h</u>	324
103	0.5	SiC / 39 B	1300	<u>5h</u>	311
106	0.5	SiC / 30 B	1300	3h	314
122	0.05	SiC / 39 B	1300	3h	398

\* B = aqueous solution of the sintering additive

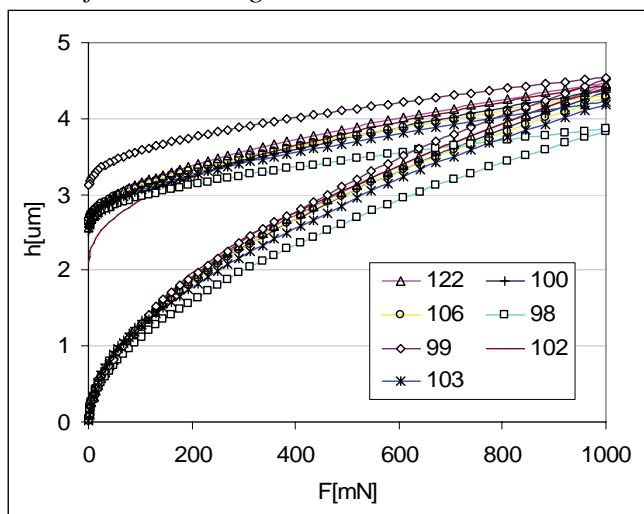


Figure 4: The change in size of indent during the indentation for different compositions

The results show that the microhardness is increases with decreasing of the sintering temperature and with the time of sintering at 1300°C. Higher values were obtained for lower amounts of the glassy phase. The microhardness for the sample with the nano-sized SiC was higher than that for the submicron-SiC.

## 2.5 Neutron irradiation performance

The starting materials, i.e. SiC powders and transient sintering additive (TSA), and sintered material for the coating were activated and their activation residuals measured at the Reactor Infrastructure Centre of the JSI. Samples were irradiated in the central channel of the TRIGA Mark II research reactor at fast neutron flux ( $E > 0.1$  MeV) of  $8 \times 10^{12}$  1/cm<sup>2</sup> s. The total neutron flux in this position was  $2 \times 10^{13}$  1/cm<sup>2</sup> s and the total neutron fluence was  $3 \times 10^{21}$  1/m<sup>2</sup>. For comparison, a sample of the commercial SiC<sub>f</sub>/SiC(CVI) was also exposed to irradiation at the same conditions.

A part of the gamma spectrum for the sample of commercial SiC<sub>f</sub>/SiC(CVI) collected one month after irradiation is presented in Figure 5. Medium and long-lived activation products (with half life values above approx. 100 days) were identified using their distinct gamma lines and half life values. As presented, the commercial sample exhibited the lowest medium and long-lived activation, which is mainly produced by <sup>51</sup>Cr, <sup>65</sup>Zn, <sup>60</sup>Co and <sup>182</sup>Ta. For both SiC powders the saturated activity results from the traces of the metals (Sc, Co and Ta), for which the amount is for an order of magnitude higher for the nano-SiC than for the submicron powder (nano-SiC has been produced by plasma-enhanced chemical vapor deposition (PECVD)). This implies that in later stage of the material development powders of better purity have to be used.

For the TSA the main cause for the measured activity were <sup>124</sup>Sb and <sup>32</sup>P. Beside the fact that the <sup>32</sup>P is a  $\beta$ -emitter, it mostly evaporates from the sample during sintering, so that the activity of the sintered sample (with submicron SiC) was similar to the activity of the starting powder. It has to be pointed out that the results presented here show the activity per gram of the coating material and not for the coated SiC/SiC (CVI).

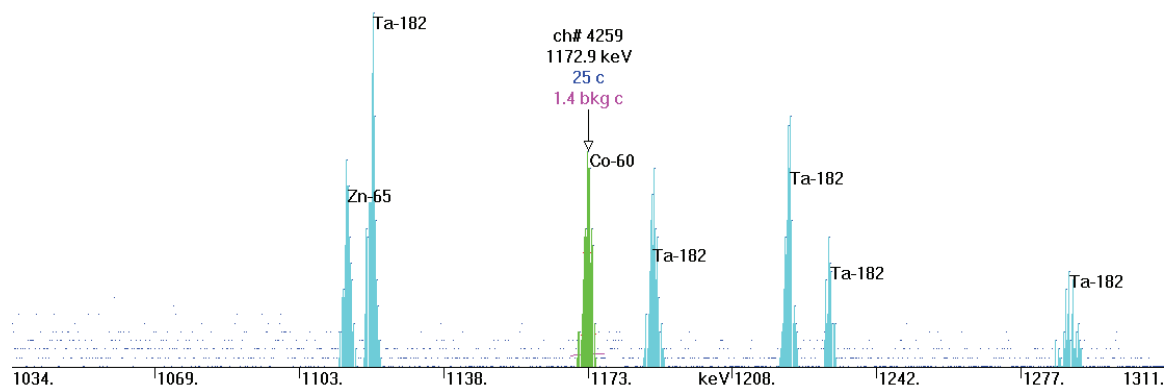


Figure 5: Gamma spectrum for the sample of commercial SiC<sub>f</sub>/SiC(CVI) collected one month after irradiation. Distinct gamma lines of <sup>65</sup>Zn (244 days), <sup>182</sup>Ta (115 days) and <sup>60</sup>Co (5.26 years) isotopes can be seen.

### 3 CONCLUSIONS AND OUTLOOK FOR 2006

- The material for the coating of the commercial SiC<sub>f</sub>/SiC composites produced by CVI was developed and two techniques for the application of the coating tested.

- Two grades of the SiC powder were used: submicron (BF12) and nano-sized (Hefei). The powders differ not only in the particle size, but also in the reactivity with oxygen as well as in impurities content and the activation after irradiation. The nano-SiC powder promises higher sinterability and is hence planned to be used as a substitute for a part of the SiC submicron powder, but needs special care in processing due to its high reactivity. In 2006, the composition of the surface layer will be analysed and tailored by using an appropriate surface modification method.

- The coating material with submicron SiC powder and addition of phosphate sintering additive enables densification of the SiC-material at temperatures from 1300 to 1500°C, providing that the process parameters are strictly controlled, in particular the atmosphere. The sintered material comprises the SiC particles with their original size and a secondary glassy phase, binding the particles. In further work, the amount of the secondary phase and its composition will be improved with the aim of improving the mechanical properties of the material and its activation behaviour.

- Due to evaporation of a part of the sintering additive during firing, the EDS analysis, XRD as well as the activation analysis reveal only a low amount of aluminum and phosphorus in the sintered materials. In continuation, the activation of the coated samples will be compared to that of the non-coated.

- The coating was applied to the SiC<sub>f</sub>/SiC composite with immersion in the SiC-based suspension or electrophoretic deposited (EPD). The latter technique appears to be promising and will be further developed in 2006. The densification process will be also studied with the aim to control the dimensional changes of the coating at the composite.

## PUBLICATIONS

### Original articles

- [1] G. Dražić, S. Novak, N. Daneu, K. Mejak, Preparation and analytical electron microscopy of SiC continuous fiber ceramic composite. *J. mater. eng. perform.*, 2005, vol. 14, p. 424-429
- [2] S. Novak, G. Dražić, K. Mejak, Electrophoretic deposition of green parts for LPS SiC-based ceramics. *Key eng. mater.*, 2006, vol. 314, pp. 45-50.

### Conference papers

- [3] G. Dražić, S. Novak, T. Toplišek, K. Mejak, Electrophoretic deposition of SiC based matrix material on SiC fibres, 41th International Conference on Microelectronics, Devices and Materials and the Workshop on Green electronics, September, 14. - September 16. 2005, Ribno, Slovenia. *Proceedings*. Ljubljana: MDEM - Society for Microelectronics, Electronic Components and Materials, 2005, p. 101-106
- [4] G. Dražić, S. Novak, T. Toplišek, K. Mejak, Analytical electron microscopy of SiC continuous-fiber ceramic composite material for fusion reactor application, *Scanning*, vol. 28, 2, p.124-125 (Proceedings of SCANNING 2006, Washington 24 - 26 April 2006)

## Novel Processing of SiC/SiC by Slip-infiltration of SiC Fibre Pre-forms with SiC under Vacuum

G. Dražić, S. Novak, T. Toplišek, K. Mejak, N. Drnovšek, T. Žagar\*

“Jožef Stefan” Institute  
Department for Nanostructured Materials  
\*Department for Reactor Physics  
Goran.Drazic@ijs.si, Sasa.Novak@ijs.si

### 1 INTRODUCTION

The basic aim of the work in this project was the substitution of the CVI technique for the preparation of SiCf/SiC composite materials with an alternative method, where the SiC-fiber preform is vacuum-infiltrated with a specially designed ceramic suspension and densified in such a way to obtain a dense and impermeable matrix with good adherence to the SiC - fibres. We proposed that the vacuum slip infiltration (VSI) method offers a more efficient way for the preparation of dense and impermeable SiC<sub>f</sub>/SiC composites with properties suitable for application in fusion reactors, without the drawbacks of the CVI technique. The study was focused on optimising the composition of the suspension and the fibre-matrix adherence.

### 2 WORK PERFORMED IN 2005

Our goal was to prepare a SiC based composite material that will meet all demands for nuclear fusion reactor application. Good high temperature mechanical properties, no open porosity, good thermal conduction and low activation in neutron flux are the main features that should be achieved. We used slip infiltration as a method of preparation of composite material and our aim was the densification of matrix SiC based material without substantial shrinkage at moderate temperatures (below 1500 °C).

#### 2.1 Optimisation of the chemical composition of the matrix material for infiltration

We used SiC-based material for the matrix where binding secondary phase enabled the densification of the material (rearrangement of primary SiC particles). During the firing process the secondary phase should have low melting temperature (below 1500 °C) and low viscosity to wet uniformly SiC particles. This phase should also enable a firm bond of matrix phase to the SiC fibres. The low-melting point secondary phase with a low high-temperature viscosity would have detrimental effects on high-temperature mechanical properties, so we investigated the possibility to use a system where the liquid phase would be just a transient one and after the densification process its properties would change to higher viscosity and higher melting point. We studied the formation of liquid phase in systems P<sub>2</sub>O<sub>5</sub>-SiO<sub>2</sub>, Al<sub>2</sub>O<sub>3</sub>-P<sub>2</sub>O<sub>5</sub>-SiO<sub>2</sub> and MgO-P<sub>2</sub>O<sub>5</sub>-SiO<sub>2</sub>. In all systems the liquid phase is formed at temperatures between 1200 and 1400 °C. After a certain amount of time at high temperature the content of P<sub>2</sub>O<sub>5</sub> decreased due to evaporation. We expect that the binding phase with a lower amount of

$P_2O_5$  should have higher melting and softening temperatures. We are trying to keep the amount of secondary phase as low as possible.

The suspensions for the infiltration were prepared by homogenization of the aqueous suspension of SiC-powder with different amounts of water solution of aluminium dihydrogen phosphate. A set of samples for the sintering studies of the matrix material and for the analysis of the material properties, were prepared by drying the suspension and subsequent sintering of the resulting powder at various temperatures in argon or nitrogen.

The starting materials were composed of SiC powder, up to 35 %  $P_2O_5$  and up to 8 % of  $Al_2O_3$ , (i.e. up to 6.14% P and 1.65 % Al). During firing, the gaseous products were evaporated from the samples which resulted in approximately 10 % of the samples weight loss. We suppose, that a major part of the  $P_2O_5$  is eliminated and reduced to phosphorus that collects at cold parts of the furnace. Hence, as will be presented later, the sintered samples contained only a very small amount of aluminium and a negligible amount of phosphorus. In further work, the composition will be further optimised with the aim to minimise Al content.

In order to effectively infiltrate SiC-fibre perform, the wettability of the slightly hydrophobic fibres has to be improved. Preliminary wetting studies showed that the wettability could be improved by adding surface active agents. According to the exhaust method we deposit on fibers the water solution of anionic surfactant Sodium dioctyl sulphosuccinate (SDOSS) and dry them at room temperature.

At this stage the samples of the composite SiCf/SiC material were prepared without any interphase between fibres and matrix which would deflect the cracks when they reach the interfacial area. Deflection of cracks would prevent catastrophic failure of the material.

## 2.2 SEM characterisation of SiC/SiC-VSI

Scanning electron microscopy was routinely used for the characterization of prepared samples with different chemical composition and amount of additives. Also for preliminary study of matrix phase, adhesion to the SiC fibres SEM is quite successful and a fast method. As an example Fig. 1 shows a low-magnification image of SiC fibers, coated with matrix material (based on 0.5 um sized SiC particles and secondary phase based on  $Al_2O_3$ - $P_2O_5$ - $SiO_2$ ). Fig. 2 shows an SEM image of SiC (500 nm sized) matrix phase, containing  $Al_2O_3$ - $P_2O_5$ - $SiO_2$  secondary phase (sintered at 1450 °C). From the image we can estimate the amount of porosity using stereology techniques. In Fig. 2 the measured porosity was 0.5+/-0.2 percent.

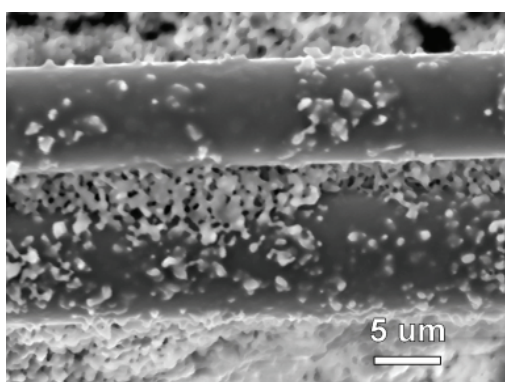


Fig. 1 SEM image of a thin layer of matrix phase on SiC fibers

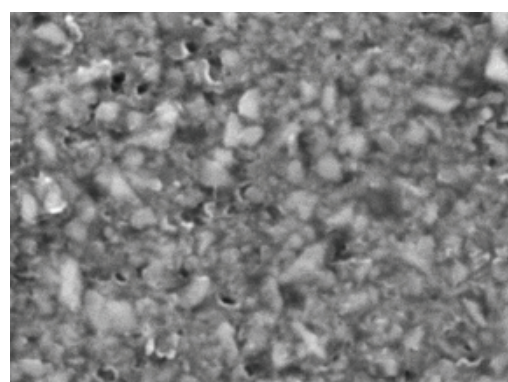


Fig. 2 SEM image of SiC/  $Al_2O_3$ - $P_2O_5$ - $SiO_2$  matrix phase

In Figure 3 the SEM image of the SiC fiber embedded in SiC based matrix material (using nano-graded starting powder) is shown. From the micrograph we could conclude that the interface between fibres and matrix is quite strong and there is no porosity present.

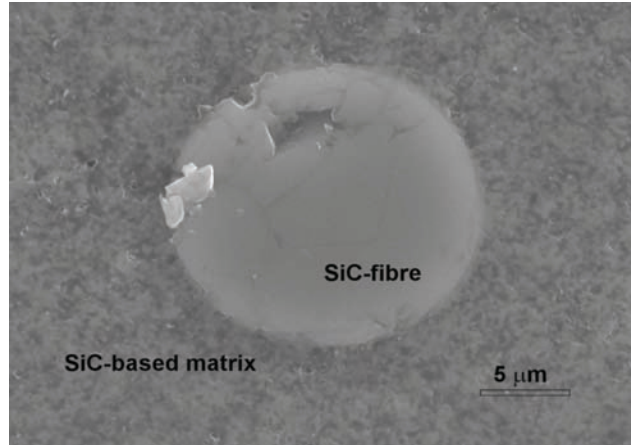


Figure 3 SEM images of the SiC fibers embedded in SiC based matrix material (using nano-graded starting powder)

### 2.3 TEM characterization of matrix and composite material

Using TEM-EDXS techniques we were studying the chemical composition and microstructure of matrix material and SiC fibre / matrix interface. As examples, Fig. 3 shows a TEM image of 20 – 50 nm sized SiC particles embedded in secondary phase. Fig.4 displays a high-resolution TEM image of an interface between two SiC nano-sized particles and a secondary phase. We found that this phase contained small amount of phosphorous and aluminium, but both in a very low concentration range. In fig. 5 an EDXS spectrum of secondary phase is shown.

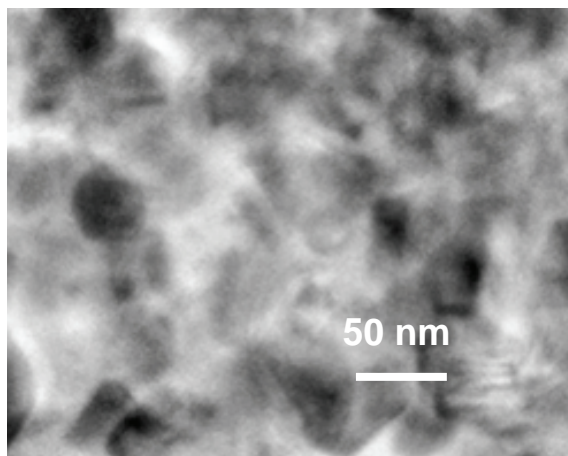


Fig. 4 TEM (bright field) micrograph of SiC/Al-Si-P-O composite

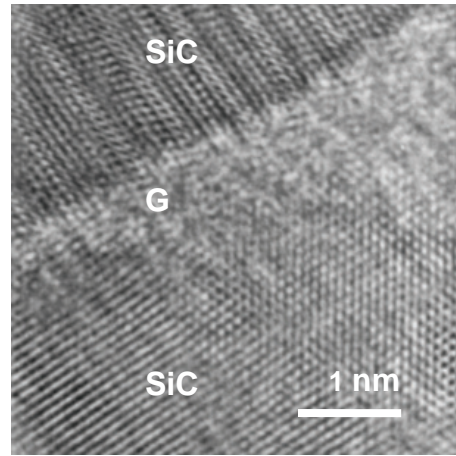


Fig. 5 HRTEM image of secondary phase (G) between two SiC particles

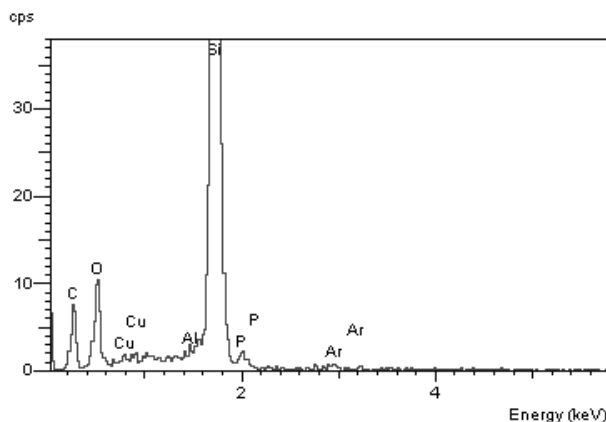


Fig. 6 EDXS spectrum of secondary phase

Analysis of the submicron-SiC powder revealed the the powder contains 1.1 wt % of oxygen, while the nano-graded SiC contains 2.4 wt %. Hence, beside introduction of oxygen in the material through sintering aids the important mechanism of incorporation of oxygen in the sintered material is through the primary SiC particles which are coated with amorphous SiO<sub>x</sub> layer.

In Fig. 7 HRTEM image of the edge of SiC particle for sub-micron graded (a.) and nano-graded (b.) SiC are shown. In both cases 1-2 nm thick oxygen containing amorphous layer was found. We expect that using non-contaminated starting chemicals, dry-boxes and working in inert atmosphere or coating the surface of the particles with a protective layer will help to reduce the oxygen content in the sintered samples..

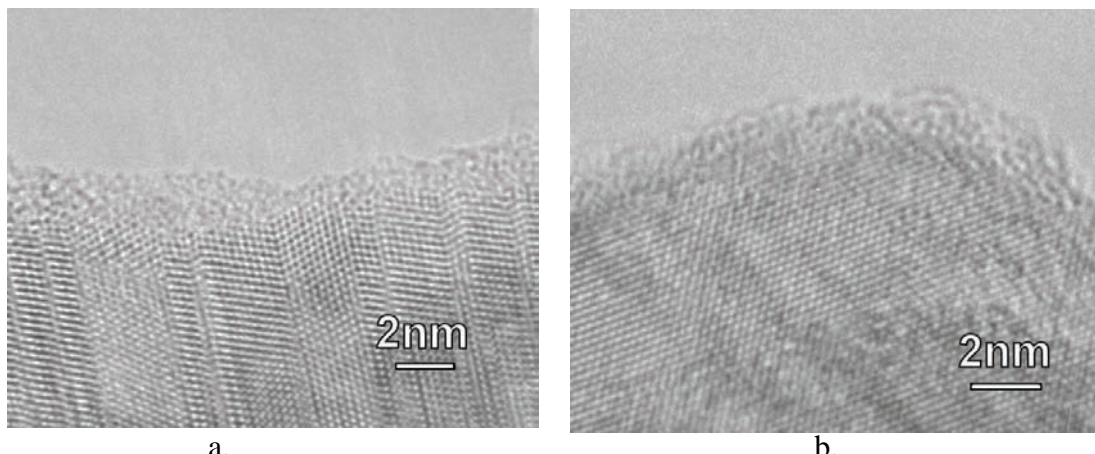


Fig. 7 HRTEM images of starting SiC particle in sub-micron graded (a.) and nano-graded (b.) silicon carbide

## 2.4 Physical characterization of matrix material

Matrix materials, prepared with different amount of additives, different grades of SiC starting powders and fired at different temperatures were analysed for densities and micro-hardness. In Table I. some of the results are listed. From the results of measurements it was concluded that, at the moment, the best results were obtained with the starting suspension of

nano-graded SiC, with the addition of 15 wt.% of aqueous solution of  $\text{Al}(\text{H}_2\text{PO}_4)_3$  and fired at 1300 °C for 2 hours.

Table I. Some results of physical measurements of matrix material

Starting composition of the suspensions	Density (g/cm3)	Microhardness (kPa)
Nano-grade SiC, 15 % $\text{Al}(\text{H}_2\text{PO}_4)_3$	1.721	400 +/- 10
Sub-micron grade SiC, 15 % $\text{Al}(\text{H}_2\text{PO}_4)_3$	1.605	350 +/- 8

## 2.5 Neutron irradiation performance

Dense matrix material and SiC/SiC composite materials were activated in fast neutron flux in the experimental fission reactor TRIGA. The measurements of activity were performed using low-background gamma spectroscopy after different cooling times. Preliminary results indicated that in overall activity impurities in the starting materials play a strong role. We found that in our samples there is the highest dose coming from impurities, such as  $^{46}\text{Sc}$ ,  $^{60}\text{Co}$  and  $^{182}\text{Ta}$ . In future the starting materials should be chosen with respect to the amount of impurities.

## 3 CONCLUSIONS AND OUTLOOK FOR 2006

The matrix material for use in SiCf/SiC composites was optimized regarding the chemical composition and firing conditions. In the future, special concern should be devoted to minimization of the oxygen content in the material. Dry-boxes and/or the use of protective coatings on SiC starting particles could solve the problem.

The chemistry of synthesis of the material was studied thoroughly using electron microcopies and microanalysis. The formation of secondary phase with higher phosphorous content at the beginning and subsequent evaporation of phosphorous pentoxyde during the thermal treatment was explained. Using special thermal treatment it would be possible to crystallize the remaining secondary phase, possibly with the addition of a small amount of seeding species.

More attention should be paid to the wettability of SiC fibers to improve the vacuum slip infiltration. SiC fibers are slightly hydrophobic and the use of a proper tenside could enhance the infiltration. Current optimized matrix material forms a rigid and compact bond with the SiC fibers by forming a reaction layer. To enhance the toughness of composite material the use of a thin interlayer film is necessary.

The first overview of the activation properties of the behaviour of the starting materials, transient sintering additive (TSA), and sintered material in neutron flux was obtained. More sample irradiations and additional gamma measurements after different cooling times (3, 6 and 12 months) are still required to fully characterize the medium and long-lived activation properties of those materials.

## PUBLICATIONS

### Original articles

- [1] G. Dražić, S. Novak, N. Daneu, K. Mejak, Preparation and analytical electron microscopy of SiC continuous fiber ceramic composite. *J. mater. eng. perform.*, 2005, vol. 14, p. 424-429
- [2] S. Novak, G. Dražić, K. Mejak, Electrophoretic deposition of green parts for LPS SiC-based ceramics. *Key eng. mater.*, 2006, vol. 314, pp. 45-50.

### Conference papers

- [3] G. Dražić, S. Novak, T. Toplišek, K. Mejak, Electrophoretic deposition of SiC based matrix material on SiC fibres, 41th International Conference on Microelectronics, Devices and Materials and the Workshop on Green electronics, September, 14. - September 16. 2005, Ribno, Slovenia. *Proceedings*. Ljubljana: MIDEM - Society for Microelectronics, Electronic Components and Materials, 2005, p. 101-106
- [4] G. Dražić, S. Novak, T. Toplišek, K. Mejak, Analytical electron microscopy of SiC continuous-fiber ceramic composite material for fusion reactor application, Scanning, vol. 28, 2, p.124-125 (Proceedings of SCANNING 2006, Washington 24 - 26 April 2006)

## 2D and 3D Deterministic Transport, Sensitivity and Uncertainty Analysis of HCPB Tritium Breeder Module Mock-up Benchmark

Ivo Kodeli, Bojan Žefran, Andrej Trkov

“Jožef Stefan” Institute

Reactor Physics Department

Andrej.Trkov@ijs.si,

### 1 INTRODUCTION

The Helium-Cooled Pebble Bed (HCPB) Breeder Blanket mock-up benchmark experiment was analysed using the deterministic transport, sensitivity and uncertainty code system in order to determine the Tritium Production Rate (TPR) in the ceramic breeder and the neutron reaction rates in beryllium, both nominal values and the corresponding uncertainties. The experiment was performed in 2005 and consists of a metallic beryllium set-up with two double layers of breeder material ( $\text{Li}_2\text{CO}_3$  powder). The reaction rate measurements include the  $\text{Li}_2\text{CO}_3$  pellets for the tritium breeding monitoring and activation foils, inserted at several axial and lateral locations in the block.

In addition to the well established and validated procedure based on the 2D code DORT, a new approach for the 3D modelling was validated based on the TORT/GRTUNCL3D transport codes. The SUSD3D code, also in 3D geometry, was used for the cross-section sensitivity and uncertainty calculations.

The TPR, the neutron activation rates and the associated uncertainties were determined using the EFF-3.0  $^9\text{Be}$  nuclear cross section and covariance data, and compared with those from other evaluations (FENDL-2.1 library). For the covariance matrices the following data were available: EFF-3 ( $^9\text{Be}$ ), IRDF-90 ( $^6\text{Li}$ ) and ENDF/B-VI ( $^7\text{Li}$ ). Sensitivity profiles and nuclear data uncertainties of the TPR and detector reaction rates with respect to the cross-sections of  $^9\text{Be}$ ,  $^6\text{Li}$ ,  $^7\text{Li}$ , O and C were determined at different positions in the experimental block.

To prepare for the design of a HCLL mock-up for neutronics studies the inventory of available cross sections, response functions and covariance matrices was done and the processing of the data performed. The available cross-section libraries include the FENDL-2 and 2.1 libraries and JEFF-3.1 data evaluations for major isotopes. In addition to the response functions from IRDF-90 the recent IRDF-2002 data were processed. Some improvements and further development of the SUSD3D cross-section sensitivity and uncertainty code were made in particular in order to facilitate the pre and post-processing. The code was upgraded from Fortran-77 to Fortran-95 concerning memory and data management. The tests of the geometry modelling requiring 3D TORT/GRTUNCL3D code system were performed, using the model (MCNP input) obtained.

### 2 HCPB BREEDER BLANKET MOCK-UP

The HCPB TBM mock-up was irradiated in the 14 MeV Frascati Neutron Generator (FNG) facility in 2005. The experimental block consists of a stainless steel (AISI-316) box

with the (x-z) cross section 31 cm x 31 cm, and 29 cm thick (y-axis). The steel box walls are 0.5 cm thick.

The box is filled with metallic beryllium and contains two double layers made of breeder material ( $\text{Li}_2\text{CO}_3$  powder). The breeder layers are 1.2 cm thick each, and are separated by 1 mm thick stainless steel walls.

Neutron spectra, tritium production rates (TPR) and detector foil activations were measured at several positions in the experimental block.

## 2.1 Discrete Ordinates Transport Calculations

Two discrete ordinates (SN) codes were used in the analyses, DORT and TORT, both part of the DOORS package.

In the DORT cylindrical model of the mock-up the breeder layers were approximated by equivalent cylinders. The sensitivity studies showed that the calculated reaction rates were not very sensitive to small variations of the size of the radius of the breeder layer cylinder. In the TORT geometrical model the breeder layers were modelled exactly. Some simplifications and differences with actual experimental design may exist due to the difficulties in reading the geometrical description from the very complex MCNP input file.

## 2.2 Results of Transport Calculations

Part of the energy range, covered by the detector, is shown in Figure 1 in terms of the so-called direct sensitivity component, or the sensitivity to the detector response functions, calculated by the SUSD3D code.

FNG TBM exp.: Sensitivity of  $\text{Au}^{197}(n,\gamma)$  reaction rate to detector response functions (direct sensitivity term).

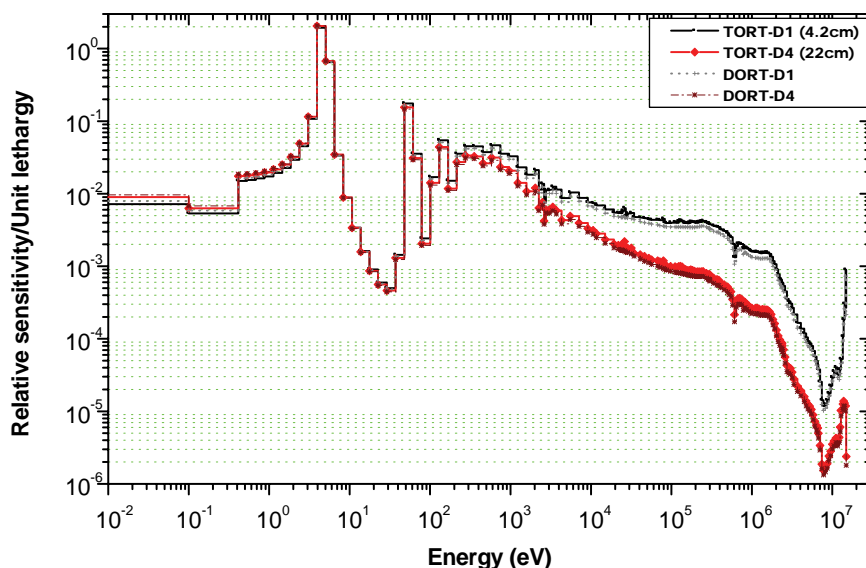


Figure 1: Sensitivity of the  $^{197}\text{Au}(n,\gamma)$  reaction to the response function for two extreme detector positions.

The results of the TORT calculational model for the detector reaction rates and the TBR in  ${}^6\text{Li}$  and  ${}^7\text{Li}$  show good consistency with the DORT results, as well as with the measured reaction rates (within 5-10 % for the reaction rates and slightly more for the TPR) which is considered reasonably good, in particular taking into account the geometrical simplifications in DORT. This agreement is considered to be largely sufficient to allow accurate sensitivity analyses, which are relative quantities and as such the agreement in energy/space distribution is more important than an agreement in the absolute values.

A  $S_{16}$  approximation was found to be required for these analyses,  $S_8$  being insufficient for the threshold detectors.

The differences between different libraries were found in general to be rather small, within a few %. The exception is  ${}^{58}\text{Ni}(n,p)$  differing by up to 8 % between calculations using EFF-3.0 and ENDL-B/VI.8  ${}^9\text{Be}$  data. Some differences were observed also for the  ${}^7\text{Li}(n,t)$  reaction.

### 2.3 Differences Between ${}^9\text{Be}$ Cross Section Evaluations

An example of the comparison of the  ${}^9\text{Be}$  cross sections from different evaluations (EFF-3.0, ENDF/B-VI and JENDL-3.3) is shown on Figure 2 for the  $(n,2n)$  reaction. FENDL-2 evaluation includes the  ${}^9\text{Be}$  data from JENDL and FENDL-2.1 from ENDF/B-VI.8 evaluation. JEFF-3.1 adopted the EFF-3.0 evaluation. Of particular importance for this study are the differences in the elastic cross section (up to 5 % around 0.1 MeV) and the  $(n, 2n)$  reaction (~5 to 10 % between ~3 and ~7 MeV).

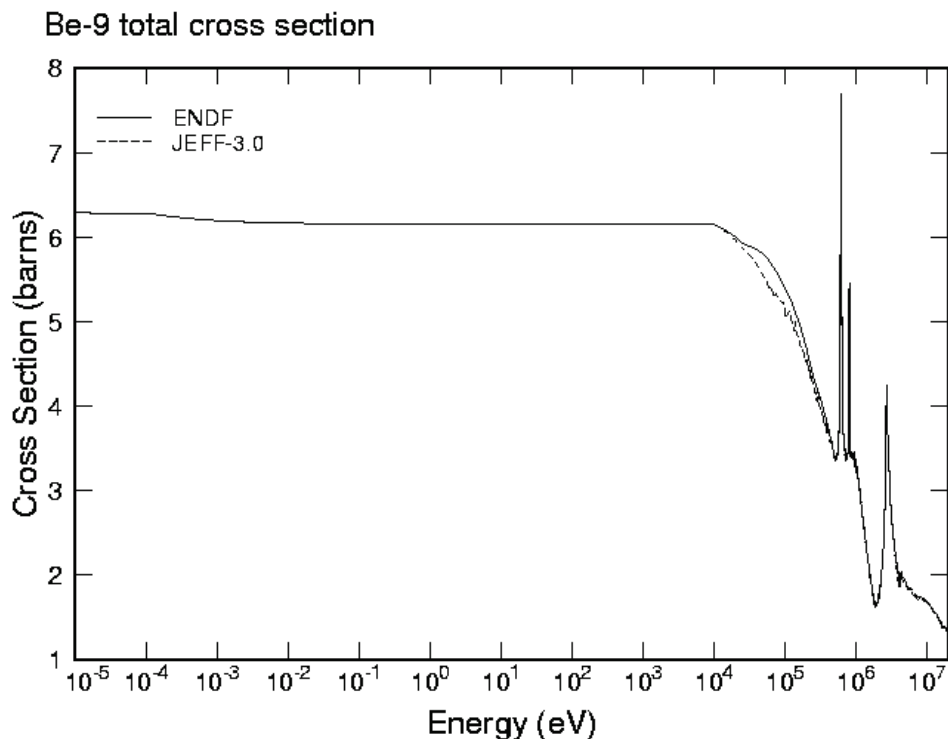


Figure 2. Comparison of the  ${}^9\text{Be}$  cross sections between different evaluations

## 2.4 SUSD3D sensitivity and uncertainty analysis

The sensitivities of the reaction rates with respect to the variations of the nuclear transport cross sections and the response functions were studied using the SUSD3D code. For these analyses the transport calculations both in the forward and adjoint mode were performed first by the DORT and TORT codes. The adjoint calculations were done using the same DORT geometrical model as for the forward calculation, but with an adjoint source, equal to the detector response functions.

Covariance matrices were taken from different origin: EFF-3 and ENDF/B-V evaluations contain matrices for  $^9\text{Be}$ ,  $^6\text{Li}$  matrices which are available in IRDF-90 and for  $^7\text{Li}$  in the ENDF/B-VI.8 evaluation.

An example of the sensitivity profiles for the TPR and reaction rates at selected positions in the mock-up with respect to the  $^9\text{Be}$  elastic cross sections is presented in Figure 3.

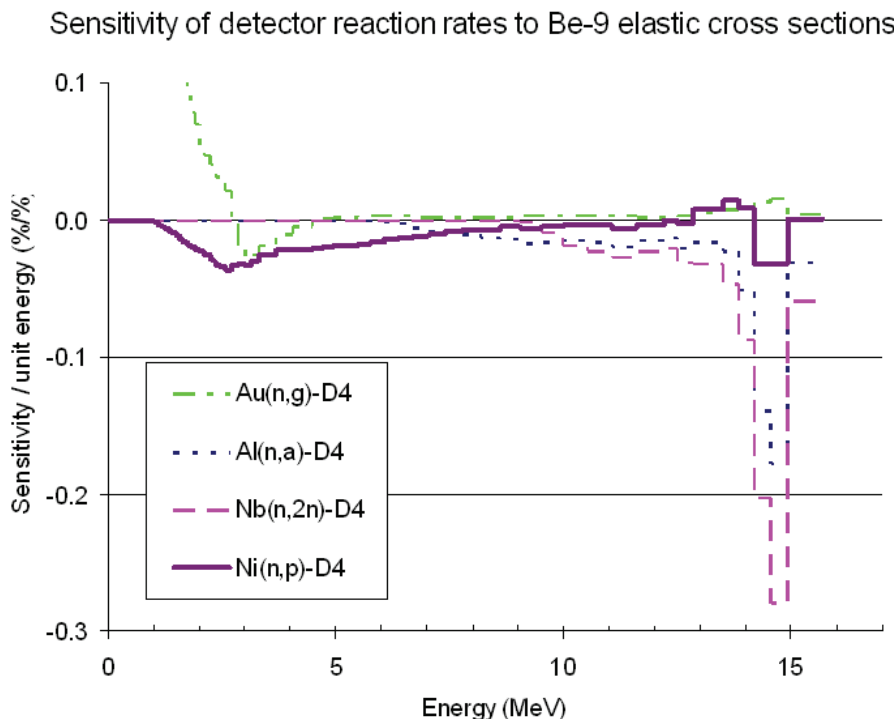


Figure 3: Sensitivity of different reaction rates to the  $^9\text{Be}$  elastic cross sections.

The main conclusions of the study are the following:

- $^6\text{Li}(n,t)$  – All reaction rates and the TPR are the most sensitive to the  $^9\text{Be}$  elastic,  $(n,2n)$ , and  $^6\text{Li}(n,\alpha)$ , cross sections. Relevant are also the  $^9\text{Be}$   $(n,t)$  and  $(n,\alpha)$ ,  $^7\text{Li}$ ,  $^{16}\text{O}$  and  $^{12}\text{C}$  cross-sections.
- According to the available covariance data the uncertainties in the tritium production rate are relatively low, between 2% (using EFF-3) and 5% (using ENDF/B-V). This does not include the uncertainties in SAD/SED for which the covariances are not available.

### 3 CONCLUSIONS

The TBM Neutronics Experiment was analysed using the deterministic code system based on the DORT and TORT particle transport codes, and the SUSD3D code for the cross section sensitivity and uncertainty analysis. The multigroup cross section data were taken from the FENDL-2 library as well as from the EFF-3 cross section evaluation. The response functions from the IRDF-2002 evaluation were used to derive the reaction rates from the calculated neutron fluxes. The covariance matrices developed in the frame of the EFF project were used. Sensitivity profiles and nuclear data uncertainties of the TPR and the detector reaction rates with respect to the cross-sections of  $^9\text{Be}$ ,  $^6\text{Li}$ ,  $^7\text{Li}$ , O and C were determined at different positions in the experimental block.

The neutron transport calculations were performed both with the 2D discrete ordinates transport code DORT as well as using a 3D code system. In this way the 3D calculations using the code TORT/GRTUNCL-3D for the transport and SUSD3D for the sensitivity and uncertainty analysis were tested against the well established 2D procedure. With the required adaptations which were introduced to the original version the 3D capability is now fully functional.

Table 1: Summary integral sensitivities and the corresponding uncertainties ( $\Delta$ ).

Elem.	Reaction	Li(n,t) TPR		$^{197}\text{Au}(n,g)$		$^{58}\text{Ni}(n,p)$	
		Sensitivity (%/%)	D (%)	Sensitivity (%/%)	D (%)	Sensitivity (%/%)	D (%)
$^9\text{Be}$	Tot	1.99	2.1 <sup>*</sup> - 5.4 <sup>#</sup>	1.9	2.1 <sup>*</sup> - 5.3 <sup>#</sup>	-0.83	1.3 <sup>*</sup> - 3.6 <sup>#</sup>
	El. (n,2n)	1.4 0.66		1.27 0.69		-0.17 -0.58	
$^6\text{Li}$	(n,at)	0.13	<0.1	-0.28	~0.1		< 0.01
$^7\text{Li}$	(n,n'at) El.	0.03 0.02	0.1	0.02	~0.1	-0.01 0.005	0.1
$^{12}\text{C}$	Tot.	0.02	0.2				
$^{16}\text{O}$	Tot.	0.04	0.2				

The main results of the sensitivity and uncertainty analysis are summarised in Table 1. The main conclusions are the following:

- DORT/GRTUNCL as well as TORT/GRTUNCL-3D results are consistent with the measurements.
- The TPR and detector reaction rate are most sensitive to the  $^9\text{Be}$  elastic, (n,2n) and  $^6\text{Li}(n,at)$  cross sections. Relevant are also the  $^9\text{Be}$  (n,t) and (n, $\alpha$ ),  $^7\text{Li}$  elastic,  $^{16}\text{O}$  and  $^{12}\text{C}$  cross-sections.
- According to EFF-3 covariance data the uncertainties in the tritium production rate are low,  $\sim 2\%$ . The ENDF/B-V covariances give an uncertainty of about 5 %. On the other hand the differences between the EFF-3.0 and ENDF/B-VI.8 or JENDL-3.3  $^9\text{Be}$  cross section evaluations at some energy ranges exceed  $2\sigma$  values of the EFF-3.0 covariances which could indicate either possible underestimation of the covariance matrices or the presence of potential problems/errors at some energies in the EFF-3.0 evaluation.

The sensitivity profiles provide also an explanation for the differences observed in the  $^{58}\text{Ni}(\text{n},\text{p})$  reaction rates between calculations using the EFF-3.0 and the ENDF/B-VI.8 cross sections.  $^{58}\text{Ni}(\text{n},\text{p})$  reaction rates are the only one of the three threshold detectors sensitive to the  $^9\text{Be}(\text{n},2\text{n})$  reaction below  $\sim 7$  MeV, where the EFF-3.0 cross sections are higher than those in the ENDF/B-VI.8. The sensitivity is negative which explains the lower Ni reaction rates calculated using the EFF-3.0 data. The better agreement with the measurements for the FENDL-2.1 data seems to suggest that the oscillations observed in the EFF-3.0 ( $\text{n},2\text{n}$ ) cross sections are unphysical.

The  $^{197}\text{Au}(\text{n},\gamma)$  reaction rate and the TPR in Li are likewise sensitive to the  $^9\text{Be}(\text{n},2\text{n})$  cross sections in the  $\sim 3$  to 8 MeV energy range. The sensitivity being positive, this should lead to a higher TPR calculated by EFF-3.0 as compared to FENDL-2.1. The positive sensitivity to the  $^9\text{Be}$  elastic cross section, with EFF-3.0 values being lower compared to FENDL-2.1/ENDF/B-VI.8 in the 0.1 MeV energy range, seems to compensate the differences in the ( $\text{n},2\text{n}$ ) reaction, leading to a rather good agreement in the TPR for this particular experimental configuration. Note that differences of the order of 5% were observed in TPR between the two libraries in the pre-analysis of this experiment, where the material concentrations and geometrical configuration were slightly different.

## PUBLICATIONS

- [1] I. Kodeli, VITAMIN-J/COVA/EFF-3 Cross-Section Covariance Matrix Library and its Use to Analyse Benchmark Experiments in SINBAD Database, *Fus. Eng. Des.* 75-79 (2005) 1021-1025
- [2] I. Kodeli, Analysis of the HCPB Breeder Blanket Mock-up Experiment for ITER Using SUSD3D Code, *International Conference "Nuclear Energy for New Europe 2005"*, Bled, Slovenia, Bled 5-8 September 2005.

## **Analysis, Design and Manufacture of Local Machining Tool (LOMAC) for Blanket Module Flexible Support Housing**

**Jože Duhovnik**

University of Ljubljana  
Faculty for Mechanical Engineering, LECAD  
joze.duhovnik@lecad.uni-lj.si.

**TRITECH d.o.o.**

Andreja Bitenca 68  
1000 Ljubljana

### **1 WORK PERFORMED IN 2005**

In year 2005 we analysed the possible requirements and usage of the proposed LOMAC tool. We have found significantly more requirements than initially envisaged. Therefore we have decided to produce two concepts, one for the outer manufacturing and the other for the inner manufacturing. The outer manufacturing represents manufacturing of the plugs from the outer side, including the vessel-wall, whereas the inner manufacturing represents manufacturing of the plugs from the inner side, including the cutting of the windings. In order to have a simpler examination, together with the IPP, we have first prepared a matrix of the manufacturing for the outer side.

A detailed composition of all important parts for the outer manufacturing has been elaborated. On the basis of the principal solutions for the details, we have performed a presentation of the object in a 3D-space. In the TRITECH company, the analysis of the details has been prepared in parallel with our presentation. The virtual presentation has been performed in the LECAD Laboratory. First data for detailed stress and deformation analyses and simulations of the manufacturing have been prepared.

The initial concept for the inner manufacturing has been completely changed because of the requirements for completely different functions and because it is not possible to assure sufficiently high accuracy in the positioning. In 2005, the concepts of the composition and details for the inner manufacturing were elaborated, as well as the 3D models for the analysis in the virtual reality.



## 5. Public Information

**Saša Novak**

Public Information, Association EURATOM-MHEST

sasa.novak@ijs.si

- **Public information materials**

3D film “Starmakers”, the brochure “Fusion Research, an Energy Option for Europe’s Future” and the panels for the FUSION EXPO were translated into the Slovenian language, edited and forwarded to printing. (*January, February 2005*)

- **Panels** for presentations of the Slovenian fusion research activities at the FUSION EXPO were edited and printed. (*March 2005*)

- **FUSION EXPO**, Ljubljana, Trg Republike 3, TR3 Building, Entrance hall/gallery; The FUSION-EXPO, an exposition on fusion research, organized within the frame of European Fusion Development Agreement and in collaboration with Slovenian Fusion Association, took place from 21 March till 31 March 2005.

Members of the Association were involved in the organization of:

- opening ceremony with European Research Commissioner Dr. Janez Potočnik,
- mounting and dismantling of the exhibition,
- guided visits for schools and other visitors,
- information for the public (internet, leaflets, etc.),
- cost statement.

All together nearly 3000 people visited the exhibition. (*March 2005*)

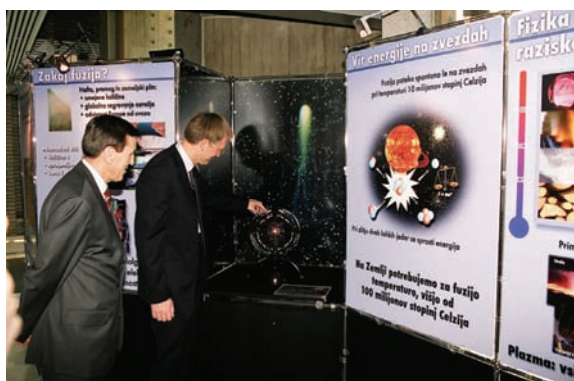


Fig. 1. Research Commissioner Potočnik at the opening of the FUSION EXPO



Fig. 2. VIPs with Assistant for PI visiting panels of the Slovenian fusion association

- **Logo** of the Slovenian Fusion Association EURATOM-MHEST prepared. (*March 2005*)

- **Contributions** to the *EFDA Newsletter* and the *IJS Newsletter* (IJS Novice) (*April 2005*)
- **Permanent EXPO at Jozef Stefan Institute**  
The panels presented at Fusion EXPO in TR3 Gallery were installed at the Jozef Stefan Institute, Nuclear Training Center in Podgorica. The exposition started in September 2005. (*August, September 2005*)
- **Fusion day** at the International Conference Nuclear Energy for New Europe 2005, September 5<sup>th</sup> to 8<sup>th</sup>, keynote lecture given by EFDA Leader M. Q. Tran, visit to the J. Stefan Institute.
- **Lecture on fusion** given at a secondary school Gimnazija Vič, by Mr. Örs Benedekfi, Hungarian Association, within a project of the quality estimation of fusion public information material. (*November 2005*)
- **Web page** of the Slovenian fusion association EURATOM-MHEST prepared and published: [www.fusion.si](http://www.fusion.si) and [www.sfa-fuzija.si](http://www.sfa-fuzija.si). (*November 2005*)



Fig. 3. Web page header of the Slovenian fusion association

- **Lectures** on fusion and fusion related materials for students at the Jozef Stefan International Postgraduate School and at the Nuclear Training Center. (*September-November 2005*)

## 6. Publications

### Scientific papers

1. GYERGYEK T., ČERČEK M.; *Sheath in front of a negatively biased collector that emits electrons and is immersed in a two electron temperature plasma,*  
Contrib. Plasma Phys., 2005, vol. 45, p. 568-581.
2. GYERGYEK T., ČERČEK M.; *Fluid model of a sheath formed in front of an electron emitting electrode immersed in a plasma with two electron temperatures.*  
Contrib. Plasma Phys., 2005, vol. 45, p. 89-110.
3. CVELBAR U., MOZETIČ M., POBERAJ I., BABIČ D., RICARD A.; *Characterization of hydrogen plasma with a fiber optics catalytic probe,*  
Thin Solid Films [Print ed.], 2005, vol. 475, p. 12-16.
4. MOZETIČ M., CVELBAR U., VESEL A., RICARD A., BABIČ D., POBERAJ I.; *A diagnostic method for real-time measurements of the density of nitrogen atoms in the postglow of an Ar-N<sub>2</sub> discharge using a catalytic probe,*  
J. Appl. Phys., 2005, vol. 97, p. 103308-1-103308-7.
5. PELICON P., RAZPET A., MARKELJ S., ČADEŽ I., BUDNAR M.; *Elastic recoil detection analysis of hydrogen with <sup>7</sup>Li ions using a polyimide foil as a thick hydrogen reference,*  
Nucl. Instrum. Methods Phys. Res., B Beam Interact. Mater. Atoms. [Print ed.], 2005, vol. 227, p. 591-596.
6. DRAŽIĆ G., NOVAK S., DANEU N., MEJAK K. *Preparation and analytical electron microscopy of SiC continuous fiber ceramic composite,*  
J. Mater. Eng. Perform., 2005, vol. 14, p. 424-429.
7. KODELI I., VITAMIN-J/COVA/EFF-3 Cross-Section Covariance Matrix Library and its Use to analyse Benchmark Experiments in SINBAD Database,  
Fus. Eng. Des. 75-79 (2005) 1021-1025.

## Conference contributions

1. ČADEŽ I., RAZPET A., PELICON P., MARKELJ S., and BREZINSEK S., *ERDA analysis of hydrogen and deuterium in the plasma-exposed graphite surfaces from the tokamak TEXTOR*, 17<sup>th</sup> International Conference on Ion Beam Analysis, June 26- July 1, 2005, Sevilla, Spain.
2. ČERČEK M., GYERGYEK T., *Double layer formation in a negative ion plasma with a bi-Maxwellian electron distribution*, 32nd EPS Conference on Plasma Physics (EPS 2005), 27 June - 1 July, 2005, Tarragona, Spain.
3. GYERGYEK T., ČERČEK M.; *Sheath formation in a two-electron temperature plasma*, 32nd EPS Conference on Plasma Physics (EPS 2005), 27 June - 1 July, 2005, Tarragona, Spain.
4. MOZETIČ, Miran, VESEL, Alenka, EVANGELAKIS, Giorgos A. *Determination of H density in a remote part of a hydrogen plasma reactor*, 32nd EPS Conference on Plasma Physics, 27th June - 1st July, 2005, Tarragona, Spain.
5. VESEL, Alenka, MOZETIČ, Miran, ZALAR, Anton. *Interaction between neutral hydrogen atoms and weakly oxidized stainless steel surface*, 32nd EPS Conference on Plasma Physics, 27th June - 1st July 2005, Tarragona, Spain.
6. GYERGYEK T., ČERČEK M.; *Sheath formation in front of a negatively biased electrode immersed in a two electron temperature plasma*, XXVIIth ICPIG, Eindhoven, the Netherlands, 18-22 July, 2005.
7. MARKELJ S., RUPNIK Z., I. ČADEŽ I., *Vibrational spectroscopy of hydrogen molecules: Extraction of hydrogen ions by field penetration technique in the presence of perpendicular magnetic field*, XXVIIth ICPIG, Eindhoven, the Netherlands, 18-22 July, 2005.
8. ČADEŽ I., RUPNIK Z. and MARKELJ S., *Cross section for dissociative electron attachment to H<sub>2</sub> and D<sub>2</sub>*, XXVIIth ICPIG, Eindhoven, the Netherlands, 18-22 July, 2005.
9. MOZETIČ M.; *Characterization of reactive plasmas with catalytic probes*, presented at 5th Asian-European International Conference on Plasma Surface Engineering, (AEPSE'2005), 12-16 September 2005, Qingdao City, China.
10. DANEU N., NOVAK S., DRAŽIĆ G., MEJAK K., *SiC continuous-fibres / SiC-based matrix composites*. V: XII. Portuguese Materials Society Meeting [and] III. International Materials Symposium, March 20 - 23, 2005, Aveiro, Portugal. Materials 2005 : program and abstract book. Aveiro: University of Aveiro, 2005, p. 200.

11. NOVAK S., DRAŽIĆ G., MAČEK S., MEJAK K.; *Electrophoretic deposition of silicon carbide*. 2nd International Conference on Electrophoretic Deposition: Fundamentals and Application : May 29 - June 2, 2005, Castelvecchio Pascoli (near Barga), Italy. Brooklyn: ECI, 2005.
12. GYERGYEK T., ČERČEK M.; *Multiple solutions for the sheath potential drop in front of a floating electron emitting collector immersed in a two electron temperature plasma*, International Conference Nuclear Energy for New Europe 2005, Bled, Slovenia, 5 - 8 September 2005.
13. MARKELJ S., RUPNIK Z. and ČADEŽ I., *Detection system for vibrational spectroscopy of hydrogen molecules for studies of collision processes in fusion edge plasma*, International Conference Nuclear Energy for New Europe 2005, Bled, Slovenia, 5 - 8 September 2005.
14. PELICON P., ČADEŽ I., MARKELJ S., SIMČIČ J., RUPNIK Z., *Analysis of materials used for plasma-facing components in tokamaks with ion beam analytical techniques*, International Conference Nuclear Energy for New Europe 2005, Bled, Slovenia, 5 - 8 September 2005.
15. MOZETIČ M., VESEL A.; *Density of neutral hydrogen atoms in a microwave hydrogen plasma reactor*, International Conference Nuclear Energy for New Europe 2005, Bled, Slovenia, 5-8 September 2005.
16. VESEL A., MOZETIČ M.; *Heterogeneous recombination of neutral hydrogen atoms on surfaces of the fusion relevant materials*, International Conference Nuclear Energy for New Europe 2005, Bled, Slovenia, 5-8 September 2005.
17. PELICON P., ČADEŽ I., MARKELJ S., SIMČIČ J., RUPNIK Z.; *Analysis of materials used for plasma-facing components in tokamaks with ion beam analytical techniques*, International Conference “Nuclear Energy for New Europe 2005”, Bled, Slovenia, 5-8 September 2005.
18. NOVAK S., DRAŽIĆ G., MEJAK K., TOPLIŠEK T., ŽAGAR T., RAVNIK M.; *Ceramic Route for fabrication on SiC/SiC composites*, International Conference “Nuclear Energy for New Europe 2005”, Bled, Slovenia, 5-8 September 2005.
19. ŽAGAR T., NOVAK S., RAVNIK M., DRAŽIĆ G.; *Neutron Activation Measurements of SiCf/SiC Composites*, International Conference “Nuclear Energy for New Europe 2005”, Bled, Slovenia, 5-8 September 2005.
20. KODELI I.; *Analysis of the HCPB Breeder Blanket Mock-up Experiment for ITER Using SUSD3D Code*, International Conference “Nuclear Energy for New Europe 2005”, Bled, Slovenia, Bled 5-8 September 2005.

21. MOZETIČ M., VESEL A.; *Heterogena rekombinacija nevtralnih vodikovih atomov na površinah materialov v fuzijskih plazemskih reaktorjih.* V: RADIĆ, Nikola (ur.). Vakuumска znanost i tehnika - 12. Međunarodni sastanak, Trakošćan, 18. maja 2005. Zbornik sažetaka. Zagreb: Hrvatsko vakuumsko društvo, 2005, str. 31.
22. DRAŽIĆ G., NOVAK S., TOPLIŠEK T., MEJAK K.; *Electrophoretic deposition of SiC based matrix material on SiC fibres,* V: MALIČ, Barbara (ur.), BELAVIČ, Darko (ur.), ŠORLI, Iztok (ur.). 41th International Conference on Microelectronics, Devices and Materials and the Workshop on Green electronics, September, 14. - September 16. 2005, Ribno, Slovenia. Proceedings. Ljubljana: MIDEM - Society for Microelectronics, Electronic Components and Materials, 2005, str. 101-106.
23. MEJAK K., NOVAK S., TOPLIŠEK T., DRAŽIĆ G., KOBE S., *Preparation of a nanostructured SiC[sub]f/SiC composite for fusion applications.* V: 4th Symposium of science and technology of nanomaterials in Slovenia, October 24th -25th, 2005, Ljubljana, Slovenia. *SLONANO 2005 : programme and book of abstracts.* Ljubljana: Jozef Stefan Institute: National Institute of Chemistry, 2005, str. 55.
24. DRAŽIĆ G., NOVAK S., TOPLIŠEK T., MEJAK K.; *Analytical electron microscopy of SiC continuous-fiber ceramic composite material for fusion reactor application,* Scanning, vol. 28, 2, p.124-125 (Proceedings of SCANNING 2006, Washington 24 - 26 April 2006)

### Public Information publications

1. ČERČEK M.; *Prvi "fuzijski" megavati do leta 2050? : fuzija - vir energije za prihodnost.* Delo (Ljubl.), 24.3.2005, str. 16, Znanost.
2. ČERČEK M.; *Raziskave fuzije v Sloveniji,* IJS Novice (IJS Newsletter) no. 118, 2005, p. 5-7
3. NOVAK S.; *Commissioner Potocnik opens Fusion Expo in Ljubljana,* EFDA Newsletter, vol. 2005/3, 2005, p. 2-3
4. NOVAK S.; *"ITER" v Sloveniji (Razstava "Fuzija, energija bodočnosti"),* IJS Novice (IJS Newsletter) no. 118, 2005, p. 2-4
5. MOZETIČ M.; *Prvi sestanek med Inštitutom "Jožef Stefan" in Raziskovalnim centrom v Jülichu v Nemčiji",* Vakuumist, 2005, vol. 25, p 34.

## Reports

1. MARKEĽ J., ČADEŽ I., PELICON P., RUPNIK Z., *In situ studies of interaction of thermal hydrogen molecules and atoms with W, graphite and some other materials:* presented at 1st Bilateral Meeting on Plasma Edge Physics and Plasma-Wall Interaction, 28-30 September, 2005, Forschungszentrum Jülich.
2. ČADEŽ I., MARKEĽ J., RUPNIK Z., ČERČEK M., GYERGYEK T., ŽIGMAN V.; *Experiments with vibrationally excited hydrogen molecules ( $H_2, D_2$ ) of relevance for edge plasmas and plasma wall interaction:* presented at 1st Bilateral Meeting on Plasma Edge Physics and Plasma-Wall Interaction, 28-30 September, 2005, Forschungszentrum Jülich.
3. ČADEŽ I. et al., *Activities relevant to PWI in fusion devices of Slovenian Fusion Association (SFA) (Association EURATOM - MHST)*: presented at 4th Meeting of EFDA Task Force for Plasma Wall Interaction, 17-19 October, 2005, Cadarache, France. 2005.

## Theses

1. MAGLICA J., *Production and characterization of hydrogen plasma*, grad. thesis, University of Ljubljana 2005, (in Slovenian).





